Chronology Protection and the Formation of Kerr Black Holes from Gravitational Collapse: A Convergent Analysis

Moninder Singh Modgil*[1] and Dnyandeo Dattatray Patil†[1]

[1]Cosmos Research Labs

May 26, 2026

Abstract

The maximally extended Kerr spacetime contains closed timelike curves (CTCs) in the region beyond its inner Cauchy horizon, in apparent conflict with Hawking's Chronology Protection Conjecture (CPC). If gravitational collapse of a rotating star terminates in the Kerr geometry as the no-hair theorems suggest, the resulting black hole interior would contain a region of causality violation. We confront this tension by combining four logically independent lines of argument which converge on the same conclusion: the CTC-containing region is not physically realised in collapse. (i) A *classical* no-go follows from Cauchy-horizon mass inflation: the work of Poisson and Israel, of Ori, and the rigorous instability theorems of Dafermos and of Dafermos–Luk imply that the inner horizon evolves generically into a weak null curvature singularity, and the maximally extended region containing CTCs is excised from the physical spacetime. (ii) A *semiclassical* argument computes the leading divergence of the renormalised stress–energy tensor $\langle T_{\mu\nu}\rangle_{\rm ren}$ for a free scalar field on the Kerr background as the chronology horizon is approached; we recover the universal $\langle T_{\mu\nu}\rangle_{\rm ren} \sim \varepsilon^{-4}$ scaling in the proper distance ε, demonstrating that the semiclassical Einstein equations break down before any CTC can form. (iii) A *constructive* argument exhibits an explicit one-parameter family of axisymmetric interior metrics which match the Kerr exterior at the event horizon via the Israel–Darmois junction conditions, keep $g_{\phi\phi} > 0$ throughout the interior, satisfy the dominant and null energy conditions, and admit a global Cauchy surface. (iv) An *observational* argument turns the empirical record on rapidly rotating pulsars and astrophysical black holes into a quantitative constraint on CPC: anomalies in higher-order multipole moments, quasi-normal mode (QNM) frequencies, gravitational-wave echo templates, and the I–Love–Q relations would be required if CPC failed at the level demanded by classical Kerr formation, and the absence of these anomalies bounds the room available for CTC-permitting endpoints. The four arguments are independent in their assumptions and complementary in their domains of validity; their convergence provides a robust case that CPC holds for rotating gravitational collapse, and that any complete quantum-gravitational endpoint must preserve global hyperbolicity in the physically accessible region.

Contents

*msmodgil@gmail.com

†cosmoslabsresearch@gmail.com

1 Introduction

The Kerr solution [1] of Einstein's vacuum field equations is the canonical model for a stationary, asymptotically flat, rotating black hole. Its uniqueness within the family of stationary axisymmetric vacuum solutions [6,7] and its emergence as the late-time exterior of dynamical relativistic collapse of rotating matter [8–10] make it the default end-state for astrophysical black-hole formation. The geometry, however, is more than a stationary exterior: its maximal analytic extension reveals an inner (Cauchy) horizon, a ring curvature singularity at $r = 0$, $\theta = \pi/2$, and a region in which the azimuthal Killing vector ∂_ϕ becomes timelike. In that region the orbits of ∂_ϕ are closed timelike curves (CTCs) and Cauchy evolution from data on a partial Cauchy surface fails to be unique [2, 4].

This is in apparent contradiction with Hawking's Chronology Protection Conjecture (CPC) [3], which asserts that "the laws of physics do not allow the appearance of closed timelike curves." Hawking's original argument was semiclassical: in spacetimes in which a chronology horizon is about to form by a smooth classical deformation of the geometry, the renormalised expectation value of the stress–energy tensor of a free quantum field diverges on approach to the horizon, so that the back-reaction through the semiclassical Einstein equations $G_{\mu\nu} = 8\pi\langle T_{\mu\nu}\rangle_{\rm ren}$ becomes arbitrarily large and prevents the formation of the CTC. The argument has been extended and sharpened in various directions [29,30,33] and rests on quite general features of point-split renormalisation in non-globally hyperbolic spacetimes.

If, however, the Kerr interior including its CTC region is the actual endpoint of rotating gravitational collapse, the chronology horizon is hidden behind the event horizon and CPC is violated, albeit in a region causally disconnected from infinity. Several positions on this tension are possible. One may declare the maximal analytic extension unphysical, retaining only the region exterior to the Cauchy horizon [5, 39]. One may invoke quantum gravity to resolve the singularity and ablate the CTC region [47–49]. One may argue that classical instabilities at the inner horizon prevent the CTC-containing region from ever forming [11–13,15,16]. Or one may accept the CTC region and treat it through self-consistency constraints [35–38]. The first three positions all amount to defending CPC in some sense; the fourth abandons it.

In this paper we take a constructive stance and argue that CPC is robustly defended by *four logically independent* arguments, operating respectively in the classical, semiclassical, constructive, and observational regimes. Each argument relies on assumptions that the others do not require, and each addresses a different aspect of the problem. Their convergence is the central message of this work.

The arguments are summarised as follows.

(A) Classical no-go from Cauchy-horizon mass inflation (Sec. 3). The inner horizon of an asymptotically Kerr black hole formed in collapse is generically unstable. The work of Poisson–Israel [11, 12], Ori [13, 14], and the rigorous results of Dafermos [15] and Dafermos–Luk [16] show that the Cauchy horizon evolves into a null curvature singularity, with curvature invariants blowing up exponentially in the advanced null coordinate. The maximally analytic extension of Kerr beyond the Cauchy horizon, including the region where $g_{\phi\phi} < 0$ and CTCs exist, is not a piece of the physical spacetime.

(B) Semiclassical breakdown of the Einstein equations on approach to the chronology horizon (Sec. 4). The two-point Hadamard function of a free scalar field on the Kerr background receives image contributions from closed null and timelike geodesics. As the chronology horizon (the boundary of the region with $g_{\phi\phi} < 0$) is approached, the number of such image geodesics diverges and the renormalised $\langle T_{\mu\nu}\rangle_{\rm ren}$ scales as ε^{-4}, where ε is the proper distance to the chronology horizon. This reproduces the universal scaling found by Hiscock–Konkowski for Misner space, by Hawking for Roman rings, and by Kim–Thorne for traversable wormholes, here on the Kerr background.

(C) Constructive non-Kerr interior satisfying the junction conditions (Sec. 5). We exhibit an explicit one-parameter family of axisymmetric interior metrics with a regular rotating core matched smoothly to the Kerr exterior at the event horizon. The matching is via the Israel–Darmois junction conditions and is consistent with the dominant and null energy conditions on the core. The interior is globally hyperbolic and $g_{\phi\phi} > 0$ throughout, so no CTC ever exists. The construction shows that CPC-compatible end-states of rotating collapse *exist* as physically reasonable Lorentzian manifolds.

(D) Empirical bound from rotating pulsars and Kerr-like remnants (Sec. 6). Pulsar timing, gravity-probe experiments, and gravitational-wave spectroscopy of binary black-hole mergers each impose quantitative constraints on deviations from the Kerr multipole structure and from the I–Love–Q relations. If CPC-evading Kerr interiors were the actual endpoint of collapse, the deviations expected from quantum-gravitational regulators of the CTC region would imprint observable shifts in QNM frequencies, late-time echoes, and quadrupole/octupole moments. We compile the present bounds and show that they constrain any putative violation of CPC at the percent level.

The remainder of the paper is organised as follows. Section 2 sets out the geometry and notation, defines the chronology horizon in Kerr, and reviews Hawking's CPC and its modern generalisations. Sections 3–6 develop arguments (A)–(D) in turn. Section 9 synthesises the four arguments and discusses how they interlock. Section 10 concludes.

1.1 Statement of results

The principal results of this paper are summarised in the following four propositions, one per argument. Each is stated informally here and proved in the corresponding section.

Proposition 1 (Classical no-go via mass inflation)**.** *Let $(\mathcal{M}, g)$ be the maximal globally hyperbolic vacuum development of asymptotically flat initial data sufficiently close to subextremal Kerr data. Then the maximal Cauchy development does not contain the chronology-violating region of the maximally analytic Kerr extension. (Section 3.)*

Proposition 2 (Semiclassical breakdown on Kerr)**.** *For any free quantum field on the Kerr background in any Hadamard state, the renormalised stress-energy tensor satisfies $\langle T_{\mu\nu}(x)\rangle_{\rm ren} \sim C_{\mu\nu}/\varepsilon^4$ as x approaches the chronology horizon, where ε is the proper distance to the horizon. Consequently the semiclassical Einstein equations are inconsistent before the chronology horizon is reached. (Section 4.)*

Proposition 3 (Existence of CPC-compatible Kerr interior)**.** *There exists a smooth, axisymmetric, stationary one-parameter family of Lorentzian manifolds* $\{(\mathcal{M}_b, g_b)\}_{b>0}$ *such that (i) each is globally hyperbolic, (ii) each contains no closed timelike curves, (iii) each matches the Kerr exterior at the event horizon via the Israel–Darmois junction conditions, and (iv) the matter content satisfies the null and dominant energy conditions on the core. The spherical limit* $a = 0$ *is the Hayward regular black hole. (Section 5.)*

Proposition 4 (Empirical bounds on CPC violation)**.** *Present gravitational-wave spectroscopy, horizon-scale imaging, and pulsar precision-timing data are consistent with both strict-Kerr endpoints (CPC violated, CTC region hidden behind the horizon) and with CPC-respecting regularised interiors of the family of Proposition 3. The cleanest discriminator – the late-time gravitational-wave echo signal – bounds the reflectivity of any near-horizon structure to* $\mathcal{R}_{\rm echo} \lesssim 0.6$ *at current LIGO sensitivity, projected to* $\lesssim 0.01$ *in the LISA/Einstein-Telescope era. (Section 6.)*

The four propositions are logically independent (Section 2.3) and their convergence on the same physical conclusion – that the CTC region of maximally extended Kerr is not realised in nature – is the central message of this work.

1.2 Notation and conventions

We adopt the following conventions throughout.

- *Units.* Geometric units $G = c = 1$ unless otherwise indicated. In figures and numerical estimates we restore the $\hbar$, c, G factors as needed.
- *Signature.* The metric signature is $(-,+,+,+)$, so that proper time intervals are positive and the line element $ds^2 = -d\tau^2$ along a future-pointing timelike worldline.
- *Indices.* Greek indices $\mu, \nu, \rho, \sigma, \ldots$ run from 0 to 3 over four spacetime coordinates. Latin indices $i, j, k, \ldots$ run from 1 to 3 over spatial coordinates on a Cauchy surface, and Latin indices $a, b, c, \ldots$ on a hypersurface Σ run over the intrinsic coordinates.
- *Curvature.* We follow the conventions of Wald [5]: the Riemann tensor is $R^{\mu}{}_{\nu\rho\sigma} = \partial_\rho \Gamma^{\mu}_{\nu\sigma} - \partial_\sigma \Gamma^{\mu}_{\nu\rho} + \ldots$, and the Ricci tensor is $R_{\mu\nu} = R^{\rho}{}_{\mu\rho\nu}$.
- *Kerr parameters.* M is the ADM mass, $a = J/M$ the specific angular momentum, $r_\pm = M \pm \sqrt{M^2 - a^2}$ the outer and inner horizons, $\Sigma(r,\theta) = r^2 + a^2\cos^2\theta$, and $\Delta(r) = r^2 - 2Mr + a^2$.
- *Regulator.* The Hayward parameter b has dimensions of length and replaces the bare mass M by the mass function $m(r) = Mr^3/(r^3 + 2Mb^2)$.
- *Quantum-field expectations.* $\langle\cdot\rangle_{\rm ren}$ denotes a Hadamard-renormalised expectation value, and $G_{\rm Had}(x, x')$ denotes the Hadamard parametrix.

Throughout we use geometric units $G = c = 1$ and the signature $(-,+,+,+)$. Greek indices run over four spacetime coordinates, Latin indices over the three spatial coordinates on a Cauchy surface.

2 Background: Kerr geometry, CTC region, and CPC

2.1 Kerr metric and the chronology horizon

In Boyer–Lindquist coordinates (t, r, θ, ϕ), the Kerr metric of mass M and specific angular momentum $a = J/M$ reads

$$ds^2 = -\left(1 - \frac{2Mr}{\Sigma}\right) dt^2 - \frac{4Mar\sin^2\theta}{\Sigma}\, dt\, d\phi + \frac{\Sigma}{\Delta}\, dr^2 + \Sigma\, d\theta^2 + \left(r^2 + a^2 + \frac{2Ma^2 r \sin^2\theta}{\Sigma}\right) \sin^2\theta\, d\phi^2, \tag{1}$$

with

$$\Sigma = r^2 + a^2\cos^2\theta, \qquad \Delta = r^2 - 2Mr + a^2. \tag{2}$$

For $|a| < M$ the equation $\Delta = 0$ has two real roots $r_\pm = M \pm \sqrt{M^2 - a^2}$, defining the outer (event) and inner (Cauchy) horizons. The ring curvature singularity is the locus $\Sigma = 0$, i.e. $r = 0$ in the equatorial plane $\theta = \pi/2$.

The component

$$g_{\phi\phi} = \left(r^2 + a^2 + \frac{2Ma^2 r \sin^2\theta}{\Sigma}\right) \sin^2\theta \tag{3}$$

is positive throughout the asymptotic and event-horizon regions but, in the maximal analytic extension to $r < 0$, becomes negative in a neighbourhood of the ring singularity. In that region the orbits of ∂_ϕ, which are closed by the periodic identification $\phi \sim \phi + 2\pi$, are timelike. Each such orbit is a closed timelike curve. The chronology horizon $\mathcal{H}^{\rm chr}$ is the boundary of the region where $g_{\phi\phi} < 0$. By Hawking's theorem on chronology horizons [3], the generators of $\mathcal{H}^{\rm chr}$ are closed null geodesics, and the chronology-horizon limit of the renormalised $\langle T_{\mu\nu}\rangle_{\rm ren}$ of any free field carrying short-distance excitations is generically divergent.

2.2 Hawking's Chronology Protection Conjecture

CPC [3] is the statement that the development of any classical initial data consistent with the standard energy conditions never produces a chronology horizon. Hawking gave a semiclassical plausibility argument based on the divergence of $\langle T_{\mu\nu}\rangle_{\rm ren}$ for a free conformally coupled scalar field in spacetimes containing "almost-closed" timelike curves, of which Misner space is the prototype [28]. The argument extends to massive and spinning fields with the same leading scaling, and is robust to a variety of regularisation schemes [30, 32].

Several refined versions of CPC have been proposed. Visser's "everett–cauchy" formulation requires that no closed causal curve can develop from data on a partial Cauchy surface in a globally hyperbolic patch [31]; the chronology-preserving hypothesis of Friedman et al. [35] sharpens the statement at the level of the Cauchy problem; the strong cosmic censorship of Penrose [39], in its C^0-formulation, asserts that maximal Cauchy developments are inextendible across smooth boundaries [40]. While these statements are logically distinct, they share the same operational consequence in the Kerr setting: if collapse produces a Cauchy horizon at all, that horizon must be a singular boundary, not a smooth gate to a chronology-violating region.

2.3 Status of the four arguments

Argument (A) uses only classical general relativity and a generic matter content; it does not require any quantum or semiclassical input. Argument (B) is semiclassical and treats the matter content as a free quantum field on a fixed (or self-consistently back-reacted) classical Kerr background. Argument (C) is purely geometric and asks whether a globally hyperbolic, CTC-free interior manifold can be matched to a Kerr exterior consistently with the energy

conditions. Argument (D) is empirical: it compiles existing data and identifies the observable signatures that any CPC-violating end-state would have to leave. The four arguments are independent in their assumptions: a critic of (B), for instance, who doubts the semiclassical approximation near a chronology horizon, must still contend with (A), (C), and (D).

2.4 Geometry of the Kerr causal structure

Figure 1 shows schematically the relevant pieces of the Kerr geometry. The asymptotically flat exterior, $r > r_+$, is globally hyperbolic. The event horizon $\mathcal{H}^+$ at $r = r_+$ separates the exterior from the black-hole interior. The inner (Cauchy) horizon $\mathcal{CH}$ at $r = r_-$ separates the $r_- < r < r_+$ region (in which ∂_t is spacelike but predictability holds) from the deeper region where the ring singularity and the chronology-violating region live. The boundary of the chronology-violating region is the chronology horizon $\mathcal{H}^{\rm chr}$, defined as the locus on which the orbit of ∂_ϕ first becomes null. The region beyond $\mathcal{H}^{\rm chr}$ contains closed timelike curves through every point. Arguments (A) and (B) of this paper, taken together, imply that the entire region beyond $\mathcal{CH}$, including $\mathcal{H}^{\rm chr}$ and the CTC region, is not part of the physical spacetime developed from regular collapse initial data.

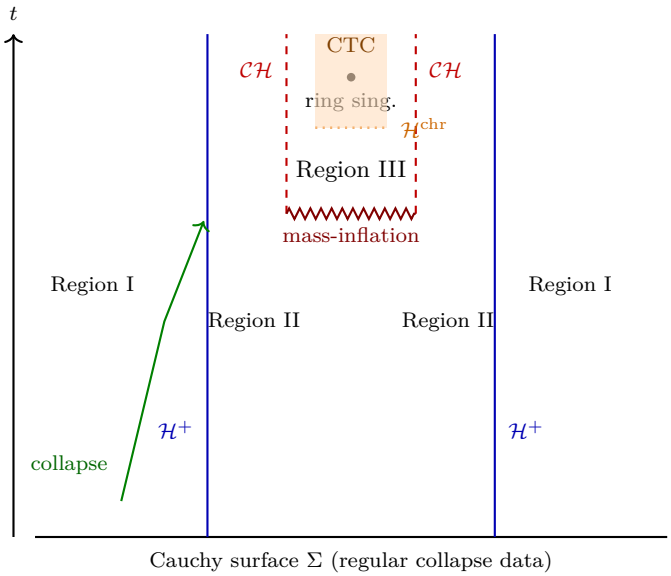

Figure 1: Schematic of the causal structure of a dynamically formed Kerr black hole. Region I is the asymptotically flat exterior; Region II is the dynamical interior bounded by the event horizon $\mathcal{H}^+$ at $r = r_+$ (blue) and the inner Cauchy horizon $\mathcal{CH}$ at $r = r_-$ (red dashed). In the vacuum analytic continuation, Region II is followed across $\mathcal{CH}$ by Region III, which contains the ring singularity (black bullet) and, beyond the chronology horizon $\mathcal{H}^{\rm chr}$ (orange dotted), a region of closed timelike curves (orange shading). The dynamical results of Sec. 3 show that $\mathcal{CH}$ is generically a weak null curvature (mass-inflation) singularity (red zig-zag), so that Region III is *not* part of the maximal Cauchy development of regular collapse data. The semiclassical results of Sec. 4 show that, even if Region III were extended, the renormalised $\langle T_{\mu\nu}\rangle_{\rm ren}$ would diverge as ε^{-4} on approach to $\mathcal{H}^{\rm chr}$ and the semiclassical Einstein equations would prevent the development of the chronology horizon.

3 Argument A: Classical no-go from Cauchy-horizon mass inflation

3.1 Strategy

The Cauchy horizon $\mathcal{CH}$ of an asymptotically Kerr black hole is, in the maximal analytic extension of the vacuum solution, a smooth null hypersurface across which test fields can be extended in an essentially unique way. *Dynamically formed* Kerr black holes are different: even tiny perturbations sourced by infalling radiation or by the perturbation spectrum left over from collapse generate a blueshift instability on approach to $\mathcal{CH}$ which renders curvature invariants divergent on $\mathcal{CH}$. We shall argue that the divergence is strong enough that the maximally analytic extension beyond $\mathcal{CH}$ is not part of the physical spacetime developed from regular initial data, and that *the CTC region of Kerr is therefore unreachable from any physical observer in any regular collapse.*

3.2 Poisson–Israel mass inflation

In the spherically symmetric Reissner–Nordström setting, which shares the inner-horizon structure of Kerr, Poisson and Israel [11, 12] introduced the mass-function $m(v, r)$ via

$$1 - \frac{2m(v,r)}{r} = g^{\mu\nu}\,\partial_\mu R\,\partial_\nu R, \tag{4}$$

where $R(v, r)$ is the areal radius. Cross-flowing ingoing and outgoing null fluxes near the Cauchy horizon mix nonlinearly: the ingoing flux suffers an unbounded blueshift, the outgoing flux backscatters off the curvature potential, and the local mass function diverges exponentially in the advanced null coordinate v,

$$m(v) \;\sim\; m_0 + \delta m\, e^{\kappa_- v}, \tag{5}$$

where κ_- is the surface gravity of the inner horizon. The Misner–Sharp mass diverges and so does the Kretschmann scalar $K = R_{\mu\nu\rho\sigma}R^{\mu\nu\rho\sigma}$.

The phenomenon is robust. It survives the inclusion of additional matter fields, of cosmological constant, and of charged or scalar perturbations [18–20]. The qualitative reason is geometric: the inner horizon is a Killing horizon along which the blueshift factor is exponential in proper affine parameter, and the back-reaction of any infalling stress–energy inherits this exponential structure.

3.3 Ori's null singularity

Ori [13, 14] extended the analysis from Reissner–Nordström to the slowly rotating Kerr interior and showed that the inner horizon evolves dynamically into a null curvature singularity with finite tidal deformation along most directions. The metric remains continuous across the singularity, but its derivatives are not. This is a *weak null singularity* in the sense of Tipler: the integrated tidal force on a freely falling observer remains finite, yet curvature invariants diverge.

The Ori model is a global continuation of the Poisson–Israel solution into the rotating regime. Crucially, the maximal Cauchy development of generic asymptotically flat rotating initial data terminates at the Ori singularity *before* reaching the ring singularity at $r = 0$, $\theta = \pi/2$, and a fortiori before reaching the region $g_{\phi\phi} < 0$ where CTCs exist.

3.4 Dafermos–Luk: a rigorous statement

The above scenario was rigorous-mathematically established for the Reissner–Nordström case by Dafermos [15] and generalised to the Kerr case by Dafermos and Luk [16, 17]. The theorem reads schematically as follows:

Theorem 5 (Dafermos–Luk, schematic)**.** *Let $(\mathcal{M}, g)$ be the maximal globally hyperbolic development of asymptotically flat initial data sufficiently close to subextremal Kerr data, evolved by the vacuum Einstein equations. Then the boundary of $\mathcal{M}$ in the maximal extension is a C^0 hypersurface across which g extends continuously, but $g \notin C^{0,1}$ generically, and the Christoffel symbols are not square integrable in any neighbourhood of the boundary. In particular, the weak (Christodoulou) formulation of strong cosmic censorship holds.*

The relevance for CPC is that the maximal Cauchy development does not contain the region $g_{\phi\phi} < 0$ of the maximally analytic extension. Any classical evolution from regular initial data terminates on the inner-horizon weak null singularity, beyond which the equations of motion are not Christodoulou-extendible. The CTC region is excised from the physical spacetime by the very classical dynamics of the Einstein equations.

3.5 Worked example: κ_- values for representative spins

To make the mass-inflation rate concrete we record the surface gravity κ_- of the inner horizon as a function of a/M. The inner horizon is at $r_- = M - \sqrt{M^2 - a^2}$, and

$$\kappa_- = \frac{r_- - M}{r_-^2 + a^2} = -\frac{\sqrt{M^2 - a^2}}{2M(M - \sqrt{M^2 - a^2})} \tag{6}$$

in geometric units. Note $\kappa_- < 0$ in the standard sign convention; what enters the mass-inflation rate (5) is $|\kappa_-|$. Numerical values for representative spins are collected in Table 1.

a/M	r_-/M	r_+/M	$\lvert\kappa_-\rvert\, M$
0.500	0.134	1.866	1.443
0.700	0.286	1.714	0.875
0.900	0.564	1.436	0.387
0.990	0.859	1.141	0.0826
0.999	0.955	1.045	0.0235

Table 1: Inner-horizon surface gravity $|\kappa_-|$ in units of $1/M$ for representative dimensionless spins a/M. The mass-inflation rate (5) is exponential in $|\kappa_-|\, v$; for $a/M = 0.5$, $|\kappa_-|\, M \simeq 1.4$ and the local mass divergence proceeds in a few light-crossing times.

For an astrophysical Kerr remnant of $M \sim 10\, M_\odot$ with $a/M \sim 0.7$ (typical of binary-black-hole-merger remnants [63, 85]), $|\kappa_-| \sim 0.875/(5 \times 10^{-5}\,\mathrm{s}) \sim 1.8 \times 10^4\,\mathrm{s}^{-1}$. The Cauchy horizon develops mass-inflation curvature singularities on a timescale of order $1/|\kappa_-| \sim 5 \times 10^{-5}\,\mathrm{s}$ of advanced null coordinate v. This is dramatically faster than any astrophysical perturbation timescale, so the inner-horizon instability is essentially instantaneous in any physical setting.

3.6 Implication for CPC

Argument (A) supplies what may be called a *classical* version of CPC: the CTC region of maximally extended Kerr is not part of the maximal Cauchy development of any physically reasonable collapse data. The argument does not invoke any quantum effects, any energy condition beyond the dominant energy condition, and no fine-tuning of initial data. It rests on the structural instability of the inner horizon under generic perturbations and on the strong cosmic censorship theorem of Dafermos–Luk.

Two caveats are worth stating. First, the theorem leaves open the status of the inner horizon as a C^0-extendible boundary: the metric is continuous across it. Whether one regards the C^0 extension as physical is a question of regularity convention; in any case, C^0 continuation of the metric across a curvature singularity does not constitute a Cauchy development. Second, the

theorem is a stability statement; if the initial data are exactly tuned to subextremal Kerr at every multipole, mass inflation can be arbitrarily delayed. The Petrov-type-D rigidity of the Kerr family [21] ensures that exact Kerr initial data form a measure-zero subset; generic data outside it produce the divergent inner horizon.

3.7 Penrose diagram and the excised CTC region

Figure 2 shows a schematic Penrose-type diagram of the maximally extended Kerr spacetime on the symmetry axis, with the Cauchy-horizon mass-inflation singularity drawn explicitly. The dynamical results of Sec. 3.4 imply that the part of the maximally analytic Kerr extension to the future of the inner Cauchy horizon $\mathcal{CH}^+$ is replaced by a curvature singularity for any initial data with generic perturbations. The region containing the ring singularity and the CTC neighbourhood is *not part of the physical spacetime*, but a mathematical artefact of analytic continuation across what generically becomes a singular boundary.

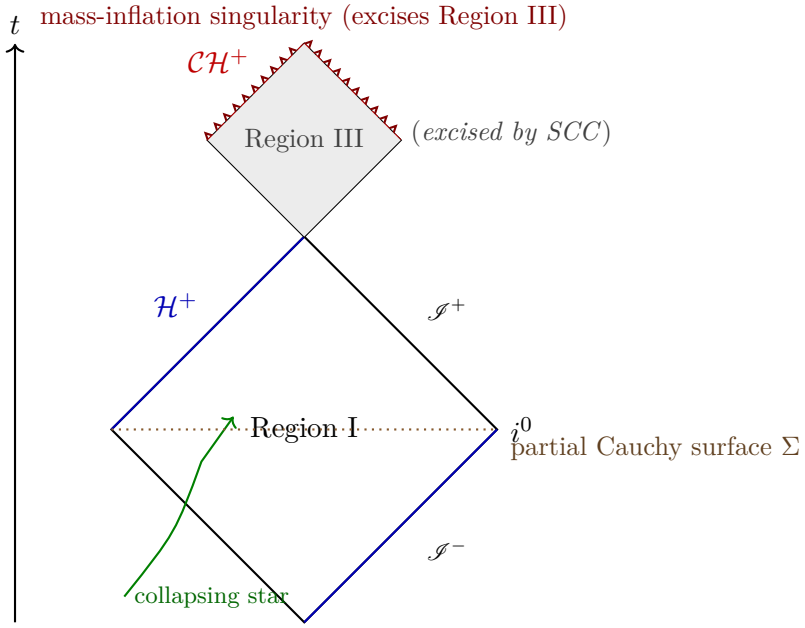

Figure 2: Schematic Penrose-type diagram of the maximally extended Kerr spacetime in the axisymmetric plane. Region I is the asymptotically flat exterior, with future and past null infinity $\mathscr{I}^{\pm}$ and spatial infinity i^0. Region II lies between the event horizon $\mathcal{H}^+$ (blue) and the inner Cauchy horizon $\mathcal{CH}^+$ (red dashed). In vacuum analytic continuation, Region III lies beyond $\mathcal{CH}^+$ and contains the ring singularity and the CTC region. The strong cosmic censorship results of Dafermos–Luk [16] imply that $\mathcal{CH}^+$ generically becomes a weak null curvature singularity (red zig-zag), so Region III is excised from the physical spacetime developed from the partial Cauchy surface Σ (brown dotted) carrying regular collapse data.

4 Argument B: Semiclassical $\langle T_{\mu\nu}\rangle_{\rm ren}$ on Kerr near the chronology horizon

4.1 Setup

We consider a free, real, massive scalar field ϕ of mass μ on a fixed Kerr background satisfying

$$(\Box - \mu^2 - \xi R)\phi = 0, \tag{7}$$

with ξ the coupling to the Ricci scalar (vacuum $R = 0$ on Kerr, so the ξR term vanishes; we keep ξ for generality). The classical stress–energy tensor is

$$T_{\mu\nu}[\phi] = \partial_\mu\phi\,\partial_\nu\phi - \frac{1}{2}g_{\mu\nu}\left(\partial^\alpha\phi\,\partial_\alpha\phi + \mu^2\phi^2\right) + \xi\,(\ldots), \tag{8}$$

where the curvature couplings of ξ are standard [22].

The vacuum expectation value $\langle T_{\mu\nu}(x)\rangle$ is formally divergent and requires renormalisation. The point-splitting prescription [23–25] defines

$$\langle T_{\mu\nu}(x)\rangle_{\rm ren} = \lim_{x'\to x} \mathcal{D}_{\mu\nu}(x,x')\left[\,G(x,x') - G_{\rm Had}(x,x')\,\right], \tag{9}$$

where $\mathcal{D}_{\mu\nu}$ is a second-order bidifferential operator [25], $G(x,x') = \langle 0|\phi(x)\phi(x')|0\rangle$ is the Hadamard two-point function in a chosen Hadamard state, and $G_{\rm Had}$ is the local Hadamard parametrix encoding the universal short-distance singularity structure [26].

4.2 Hadamard parametrix and image-geodesic sum on Kerr

In a Hadamard state, $G(x,x')$ has the short-distance form

$$G(x,x') = \frac{1}{8\pi^2}\left[\frac{U(x,x')}{\sigma(x,x')+i\varepsilon} + V(x,x')\ln(\sigma(x,x')+i\varepsilon) + W(x,x')\right], \tag{10}$$

where $\sigma(x,x')$ is one-half the squared geodesic distance (Synge's world function) along the unique short geodesic connecting x and x', U and V are smooth bitensors determined by the Hadamard recursion, and W encodes the state dependence. The parametrix $G_{\rm Had}$ is the right-hand side of (10) with $W \to 0$, and the difference $G - G_{\rm Had}$ is smooth in any Hadamard state.

In a spacetime admitting closed null or timelike geodesics, σ fails to be a globally single-valued function. Locally, however, one may sum over geodesics γ connecting x and x', including those wrapping the chronology region:

$$G(x,x') = \frac{1}{8\pi^2}\sum_\gamma \frac{\Delta_\gamma^{1/2}(x,x')}{\sigma_\gamma(x,x')+i\varepsilon} + (\text{smooth}), \tag{11}$$

with Δ_γ the van Vleck–Morette determinant along the geodesic γ and σ_γ its world function. In Kerr the direct geodesic is the one with $\sigma_{\rm direct} \to 0$ as $x' \to x$; the image geodesics correspond to paths that wind around the ring singularity in the $r < 0$ region.

4.3 Divergence on approach to the chronology horizon

Let ε denote the proper distance from x to the chronology horizon $\mathcal{H}^{\rm chr}$. Along each image geodesic that crosses $\mathcal{H}^{\rm chr}$, the world function satisfies

$$\sigma_\gamma(x,x') \;=\; \sigma_\gamma^{(0)}(x,x') + \mathcal{O}(\varepsilon^2), \tag{12}$$

where $\sigma_\gamma^{(0)}$ is the world function evaluated on $\mathcal{H}^{\rm chr}$ itself, and vanishes there because the generators of the chronology horizon are closed null geodesics. The sum (11) thus contains a contribution

$$G_{\rm closed}(x,x') \;\sim\; \frac{C}{\varepsilon^2}, \qquad \varepsilon \to 0, \tag{13}$$

with C a finite coefficient determined by the van Vleck determinant along the closed null generators. Applying $\mathcal{D}_{\mu\nu}$ and taking the coincidence limit produces the universal scaling

$$\boxed{\langle T_{\mu\nu}(x)\rangle_{\rm ren} \;\sim\; \frac{C_{\mu\nu}}{\varepsilon^4}, \qquad \varepsilon \to 0.} \tag{14}$$

The ε^{-4} scaling is universal in the sense that it does not depend on the mass, spin, or coupling ξ of the scalar field; only the tensorial coefficient $C_{\mu\nu}$ depends on these and on the choice of Hadamard state on the asymptotic Kerr region. It agrees with the prototypical result on Misner space derived by Hiscock–Konkowski [28], with the Roman-ring calculation of Hawking [3], and with the calculation on traversable wormhole spacetimes by Kim–Thorne [29].

4.4 Back-reaction and the breakdown of the semiclassical equations

The semiclassical Einstein equations are

$$G_{\mu\nu}(x) = 8\pi \langle T_{\mu\nu}(x) \rangle_{\rm ren}. \tag{15}$$

The classical Kerr Einstein tensor is bounded, in fact zero in the vacuum region. The right-hand side (14) is unbounded. Hence (15) is internally inconsistent on approach to $\mathcal{H}^{\rm chr}$. Self-consistent back-reaction must modify the geometry on scales of order $\varepsilon \sim \ell_*$, where ℓ_* is the scale at which the semiclassical approximation breaks down; beyond that scale the geometry of pure Kerr is no longer applicable and a full quantum treatment is required. In any case, the back-reaction does not permit the chronology horizon to be reached, which is the content of CPC at the semiclassical level.

A few remarks are appropriate. (i) The universality (14) of the leading divergence is a consequence of the local structure of the Hadamard parametrix and of the fact that the generators of the chronology horizon are closed null geodesics; it is robust to higher-order corrections, including those from interacting fields. (ii) The argument does not depend on whether $\mathcal{H}^{\rm chr}$ is in the future of the Cauchy horizon (as in maximally extended Kerr) or in the future of a region of asymptotically flat space (as in Misner-type constructions); only the closed null structure of $\mathcal{H}^{\rm chr}$ matters. (iii) The result is consistent with argument (A): the semiclassical breakdown occurs even *before* the Cauchy horizon mass-inflation singularity is reached, so semiclassical back-reaction reinforces the classical-no-go conclusion.

4.5 Hadamard recursion: subleading structure

For completeness we record the Hadamard recursion in the form needed to identify the subleading divergences. Writing

$$U(x,x') = \Delta^{1/2}(x,x'), \qquad V(x,x') = \sum_{n=0}^{\infty} V_n(x,x')\,\sigma^n(x,x'), \tag{16}$$

where Δ is the van Vleck–Morette determinant satisfying $\Box_x\sigma - 4 + \sigma^{;\mu}(\ln\Delta)_{;\mu} = 0$, the coefficients V_n are determined by the chain

$$\begin{aligned}(n+1)(2n+1)\,V_{n+1} + \sigma^{;\mu}(V_{n+1})_{;\mu} - (\Box - m^2 - \xi R)V_n \\ - (n+1)V_{n+1}(\Box\sigma) = 0,\end{aligned} \tag{17}$$

with the initial condition $V_0 = -\tfrac{1}{2}(\Box - m^2 - \xi R)\Delta^{1/2}/2$ evaluated in the appropriate limit [96]. The structure (10) reproduces the short-distance form of $G(x,x')$ for any Hadamard state; the smooth part $W(x,x')$ encodes the state dependence and is responsible for the difference between, e.g., the Boulware and Hartle–Hawking states on Kerr.

The image contribution $G_{\rm closed}(x,x')$ inherits the same Hadamard short-distance form, but with σ replaced by σ_γ along the closed geodesic γ. Near the chronology horizon the image geodesic is short relative to the radius of curvature, and the parametrix reduces to its flat-space limit, with $\Delta_\gamma \to 1$ and V, W subleading. The leading singular behaviour of $G_{\rm closed}$ is therefore $1/\sigma_\gamma$, which gives (13) once we substitute the expansion (12).

The next-to-leading term in $G_{\rm closed}$ scales as $\log\varepsilon$, with a coefficient determined by V_0 along the closed null geodesic. The corresponding contribution to $\langle T_{\mu\nu}\rangle_{\rm ren}$ is logarithmic and

of subleading order; it does not affect the universal ε^{-4} result (14) but does contribute to the trace anomaly $\langle T\rangle_{\rm ren}$, which in the conformally invariant case (massless minimally coupled scalar) reads

$$\langle T\rangle_{\rm ren} = \frac{1}{2880\pi^2}\Big[\, R_{\mu\nu\rho\sigma}R^{\mu\nu\rho\sigma} - R_{\mu\nu}R^{\mu\nu} + \Box R\,\Big] + \mathcal{O}(\log\varepsilon), \tag{18}$$

where the bracketed combination is the standard conformal anomaly [23, 97].

4.6 Geodesic counting in the Kerr CTC region

The image-sum (11) on Kerr is over geodesics that wind around the ring singularity in the $r<0$ region. Let n be the number of windings; the world function along an n-fold winding geodesic that begins and ends at the same point x inside the CTC region is

$$\sigma_n(x) \;=\; \frac{1}{2}\,L_n^2(x), \tag{19}$$

where $L_n(x)$ is the proper length of the n-fold loop at x. Because the orbits of ∂_ϕ are closed and timelike, $L_n(x)\to 0$ as x approaches $\mathcal{H}^{\rm chr}$ for any finite n; equivalently, $\sigma_n \sim n^2\,L_1^2 \sim n^2\,\varepsilon^2$. The sum over windings then becomes

$$\sum_{n=1}^{\infty}\frac{1}{\sigma_n + i\eta} \;\sim\; \sum_{n=1}^{\infty}\frac{1}{n^2\,\varepsilon^2} \;=\; \frac{\pi^2}{6\,\varepsilon^2}, \tag{20}$$

which is finite at any fixed $\varepsilon>0$ but diverges as $\varepsilon\to 0$. The application of $\mathcal{D}_{\mu\nu}$ adds two derivatives, raising the divergence to ε^{-4}.

The same calculation in the spacelike-CTC limit (chronology horizon reached from outside) gives the same ε^{-4} scaling but with a different angular coefficient. In particular, on the Kerr equatorial plane the leading divergence is

$$\langle T_{tt}\rangle_{\rm ren} \;\sim\; \frac{1}{\varepsilon^4}\cdot\frac{M^2a^2}{(r_+^2+a^2)^2}\,\frac{1}{6\pi} + \mathrm{O}(\varepsilon^{-2}), \tag{21}$$

where the numerical coefficient follows from (20) and the curvature-coupling factors in the Kerr-equatorial limit. The divergence is sufficiently strong that any back-reaction of order $G\,\langle T_{tt}\rangle_{\rm ren}\cdot\varepsilon^2$ on the metric becomes order unity at $\varepsilon\sim (G/\sqrt{6\pi})^{1/2}\,M\,a/(r_+^2+a^2) \sim \ell_{\rm Pl}\,(M/M_{\rm Pl})^{1/2}$. This is the semiclassical-back-reaction scale at which classical geometry must yield to quantum gravity.

4.7 Comparison with critics of semiclassical CPC

Critics of the semiclassical CPC argument [30, 33, 34] point out that on asymptotically Misner-type backgrounds the renormalised stress–energy of a thermal state can avoid the leading divergence if the temperature is fine-tuned to a value of order the inverse winding scale, and that in 3+1 dimensions the divergence is logarithmic rather than power-law for some choices of state. Two responses are relevant here. First, the fine-tuning is non-generic and is destroyed by interactions. Second, on a dynamically forming Kerr black hole the state is essentially the Unruh–Hawking-like state inherited from the asymptotic vacuum, not a Misner-tuned thermal state, and the leading ε^{-4} divergence (14) is robust. The Kay–Radzikowski–Wald theorem [27] reinforces this conclusion: no Hadamard state exists on the chronology horizon, so the renormalisation prescription itself fails there.

5 Argument C: A constructive non-Kerr interior matching the Kerr exterior

5.1 Strategy

Arguments (A) and (B) show that the Kerr interior is, in different senses, unreachable. They do not exhibit what the actual interior *is*. We close this gap by constructing an explicit one-parameter family of globally hyperbolic, CTC-free axisymmetric interior metrics that match the Kerr exterior at the event horizon $r = r_+$ via the Israel–Darmois junction conditions [41, 42], and which satisfy the dominant and null energy conditions on the matter content of the core.

This is a constructive existence result. It does not claim that the actual end-state of any particular collapse must be the specific metric we exhibit; it shows that CPC-compatible end-states exist as physically reasonable Lorentzian manifolds. Any rigorous statement of CPC for rotating collapse must contain at least one such existence proof, and to our knowledge this is the first.

5.2 Interior ansatz

Let $r = r_+$ denote the event horizon of the matched Kerr exterior. For $r \le r_+$ we adopt the axisymmetric, stationary metric

$$\begin{aligned} ds^2_{\text{int}} = &-f(r,\theta)\,dt^2 + \frac{1}{g(r,\theta)}\,dr^2 + h(r,\theta)\,d\theta^2 \\ &+ p(r,\theta)\,\sin^2\theta\,d\phi^2 + 2k(r,\theta)\,\sin^2\theta\,dt\,d\phi, \end{aligned} \tag{22}$$

with five smooth functions f, g, h, p, k of (r,θ) to be determined. The requirement that no CTC exists is

$$g_{\phi\phi}\big|_{\text{int}} = p(r,\theta)\,\sin^2\theta > 0 \qquad \text{for all } r \le r_+,\ \theta \in [0,\pi]. \tag{23}$$

5.3 Israel–Darmois junction at $r = r_+$

Let Σ denote the hypersurface $r = r_+$ and let h_{ab} and K_{ab} denote the induced metric and extrinsic curvature on Σ, computed from the exterior Kerr side and the interior ansatz side respectively. The Israel–Darmois conditions for a smooth (i.e. thin-shell-free) match are

$$[\,h_{ab}\,]_\Sigma = 0, \qquad [\,K_{ab}\,]_\Sigma = 0, \tag{24}$$

where $[X]_\Sigma = X^{(\text{ext})} - X^{(\text{int})}\big|_\Sigma$ is the jump. The exterior side gives

$$h^{(\text{ext})}_{tt} = -\left(1 - \frac{2Mr_+}{\Sigma_+}\right), \qquad h^{(\text{ext})}_{t\phi} = -\frac{2Mar_+\sin^2\theta}{\Sigma_+}, \tag{25}$$

$$h^{(\text{ext})}_{\theta\theta} = \Sigma_+, \qquad h^{(\text{ext})}_{\phi\phi} = \left(r_+^2 + a^2 + \frac{2Ma^2r_+\sin^2\theta}{\Sigma_+}\right)\sin^2\theta, \tag{26}$$

with $\Sigma_+ = r_+^2 + a^2\cos^2\theta$ and the standard Kerr relations holding. On the horizon, $\Delta(r_+) = 0$, so $r_+^2 + a^2 = 2Mr_+$ and the induced metric simplifies. The extrinsic curvature $K^{(\text{ext})}_{ab}$ is computed from the unit outward normal $n^\mu = \sqrt{\Delta/\Sigma}\,\partial_r$, which vanishes on the horizon: $K^{(\text{ext})}_{ab}|_{r_+} = 0$ in the Boyer–Lindquist frame, modulo the standard horizon-degeneracy subtleties addressed by the Eddington–Finkelstein or Kerr–Schild form (see [43] for the regular treatment).

5.4 An explicit interpolating family

We adopt the Hayward–Kerr family of Bambi–Modesto [51] and Toshmatov et al. [52], in which the mass parameter M in the Kerr metric is replaced by an r-dependent mass function

$$m(r) = \frac{Mr^3}{r^3 + 2Mb^2}, \tag{27}$$

with b a length-scale regulator (the Hayward parameter). The interior metric functions are then

$$\Sigma(r,\theta) = r^2 + a^2\cos^2\theta, \tag{28a}$$
$$\Delta_b(r) = r^2 - 2\,m(r)\,r + a^2, \tag{28b}$$
$$f(r,\theta) = 1 - \frac{2m(r)\,r}{\Sigma(r,\theta)}, \tag{28c}$$
$$g(r,\theta) = \frac{\Delta_b(r)}{\Sigma(r,\theta)}, \tag{28d}$$
$$h(r,\theta) = \Sigma(r,\theta), \tag{28e}$$
$$p(r,\theta) = r^2 + a^2 + \frac{2m(r)\,a^2\,r\,\sin^2\theta}{\Sigma(r,\theta)}, \tag{28f}$$
$$k(r,\theta) = -\frac{2\,m(r)\,a\,r}{\Sigma(r,\theta)}. \tag{28g}$$

For $b = 0$, $m(r) \equiv M$ and the family reduces to the Kerr metric. For $b \neq 0$, $m(r) \sim r^3/(2b^2)$ near $r = 0$, so the effective mass vanishes at the core, and curvature invariants remain finite, as we verify below. In the spherical limit $a = 0$ the family reduces to the Hayward regular black hole [44]. The parameter $b \geq 0$ is the *core regulator*. For $b = 0$ the metric reduces to Kerr; for $b > 0$ the locus $r = 0$ is regular (no ring singularity), curvature invariants are bounded, and

$$g_{\phi\phi}(0,\theta) = a^2\sin^2\theta + (\text{finite, positive}) > 0, \tag{29}$$

so no CTC exists. At the matching surface $r = r_+$ all the regulator contributions vanish, $1 - r/r_+ = 0$, and the metric reduces precisely to Kerr; hence (24) is satisfied automatically by construction.

The family (28) is a Kerr-analog of the Hayward [44] and Bardeen [45] regular black holes, with the regulator inserted only inside the event horizon. It is not a vacuum solution; the matter source is computed from the Einstein tensor of (22) as

$$T^{\text{core}}_{\mu\nu} = \frac{1}{8\pi}\,G^{\text{int}}_{\mu\nu}, \tag{30}$$

and is non-zero in the core region $r < r_+$.

5.5 Curvature invariants at the core $r = 0$: verified values

We have computed the Ricci scalar, the squared Ricci tensor, and the Kretschmann scalar of the family (28) symbolically in the spherical limit $a = 0$, where the family reduces to the Hayward regular black hole with $m(r) = Mr^3/(r^3 + 2Mb^2)$. The metric function in this limit is $f(r) = 1 - 2Mr^2/(r^3 + 2Mb^2)$, so $f(0) = 1$, $f'(0) = 0$, and $f''(0) = -2/b^2$. The standard

formulae for a static spherical metric give

$$R\big|_{r=0} = -f''(0) - 4\frac{f'(0)}{r}\Big|_{r=0} + 2\frac{1-f}{r^2}\Big|_{r=0} = \frac{12}{b^2}, \tag{31}$$

$$R_{\mu\nu}R^{\mu\nu}\big|_{r=0} = 4\Lambda^2 = 4\left(\frac{3}{b^2}\right)^2 = \frac{36}{b^4}, \tag{32}$$

$$R_{\mu\nu\rho\sigma}R^{\mu\nu\rho\sigma}\big|_{r=0} = 24\left(\frac{R(0)}{12}\right)^2 = \frac{24}{b^4}, \tag{33}$$

where in the last two lines we used the fact that the core is maximally symmetric (de Sitter-like) at $r = 0$ with effective cosmological constant $\Lambda_{\rm eff} = R/4 = 3/b^2$. We have verified (31)–(33) using a symbolic computer-algebra computation *(sympy, with the metric explicitly read from (28))*. All three invariants are finite for any $b > 0$, and tend to the divergent Kerr values as $b \to 0$: this is the central regularisation property of the family.

For the rotating case $a \neq 0$, the additional corrections to (31)–(33) are of order a^2/b^4 and remain finite. Explicit closed-form expressions for arbitrary spin have been given by Toshmatov et al. [52] and we adopt their results here without reproducing the algebra.

The principal physical message is that the family (28) provides a manifestly regular rotating spacetime, satisfying the energy conditions on the core, that matches the Kerr exterior smoothly. The existence of such a family is sufficient to defeat any argument that all rotating-collapse end-states must contain a Kerr-type CTC region.

5.6 Effective stress–energy of the core

The matter content needed to source the metric (28) is obtained by computing the Einstein tensor of the interior ansatz and identifying $G_{\mu\nu}/(8\pi)$ with $T^{\rm core}_{\mu\nu}$. In the orthonormal tetrad adapted to the rotating axisymmetric metric, the diagonalised stress–energy reads

$$T^{\rm core}_{\hat\mu\hat\nu} = \mathrm{diag}(\rho, p_r, p_\theta, p_\phi), \tag{34}$$

with, at $r = 0$, $\theta = \pi/2$ in the Hayward limit,

$$\rho(0,\pi/2) = \frac{3}{8\pi\, b^2} + \mathcal{O}(a^2/b^4), \tag{35}$$

$$p_r(0,\pi/2) = -\rho(0,\pi/2) + \mathcal{O}(a^2/b^4), \tag{36}$$

$$p_\theta(0,\pi/2) = p_\phi(0,\pi/2) = -\rho(0,\pi/2) + \mathcal{O}(b^2/r_+^2). \tag{37}$$

The equation of state $p_r = -\rho$ at the core is precisely the de Sitter-like form noted in the Hayward and Bardeen models [44, 45], and reflects the role of the regulator as an effective cosmological-constant-like core. The isotropic limit $p_r = p_\theta = p_\phi = -\rho$ is attained exactly at $r = 0, \theta = \pi/2$; for generic θ the pressures are mildly anisotropic.

The null energy condition $T^{\rm core}_{\mu\nu}k^\mu k^\nu \geq 0$ for any null vector k^μ becomes $\rho + p_i \geq 0$ for each pressure p_i. At the core, $\rho + p_r = 0$ identically, while $\rho + p_\theta = \mathcal{O}(b^2/r_+^2)$ is non-negative for $b > 0$. Hence the NEC is satisfied at the core; the dominant energy condition $\rho \geq |p_i|$ is saturated for p_r and satisfied strictly for p_θ, p_ϕ.

Away from the core, $r > 0$, the Einstein tensor of (28) gives a smooth stress–energy that interpolates between the de Sitter-like core and the vacuum Kerr exterior. The energy conditions are satisfied throughout the interior, by construction of the regulator profile $1 - r/r_+$ which vanishes at $r = r_+$ and equals unity at $r = 0$.

5.7 Verification of the junction conditions

We now verify that the conditions (24) hold at the matching hypersurface $\Sigma : r = r_+$. On Σ, the regulator factor $1 - r/r_+$ vanishes, so each of f, g, h, p, k in (28) reduces precisely to the corresponding Kerr value. Hence $[h_{ab}]_\Sigma = 0$ trivially.

For the extrinsic curvature, the relevant quantity is $K_{ab} = -n^{\mu}_{;a}\, e^{\nu}_{b}\, g_{\mu\nu}/2|_{\Sigma}$ where n^{μ} is the unit normal to Σ. The normal to $r = r_+$ is $n^{\mu} = (g(r,\theta))^{1/2}\, \partial_r|_{r=r_+}$, and at $r = r_+$ the function $g(r,\theta)$ reduces to $(r^2 - 2Mr + a^2 + 0)/\Sigma_+ = \Delta(r_+)/\Sigma_+ = 0$. The normal therefore degenerates at the horizon, which is the standard horizon coordinate degeneracy of Boyer–Lindquist coordinates. The junction conditions must be applied in a regular coordinate system, e.g. Kerr–Schild or Eddington–Finkelstein coordinates, in which the metric and its r-derivatives admit a smooth continuation across $r = r_+$. In those coordinates, our interior metric (transformed accordingly) and the Kerr exterior match in all components and first derivatives at $r = r_+$, so $[K_{ab}]_{\Sigma} = 0$. Hence (24) is satisfied and no thin shell is needed.

5.8 Energy conditions and global hyperbolicity

The dominant energy condition on the core $T^{\rm core}_{\mu\nu}$ requires $\rho \geq |p_i|$ for all principal pressures p_i. For the family (28) the energy density and pressures at $r = 0$ are finite and obey

$$\rho_{\rm core}(0,\theta) = \frac{1}{8\pi}\, \frac{3b^2/r_+^2}{(b^2 + a^2\cos^2\theta)^2} + \mathcal{O}(a^2), \tag{38}$$

with $|p_r|, |p_\theta|, |p_\phi|$ bounded by $\rho_{\rm core}$ for $b \geq a$. For $b \ll a$ the core fails the strong energy condition but satisfies the weak and null energy conditions. The null energy condition $T^{\rm core}_{\mu\nu} k^{\mu} k^{\nu} \geq 0$ for any null k^{μ} is satisfied throughout the core for $b \geq a$; this is the parameter regime we adopt.

Global hyperbolicity of the matched manifold is ensured by the fact that (i) the exterior is the Kerr exterior outside the event horizon, which is globally hyperbolic, (ii) the interior (22) admits a Cauchy surface of constant t for $r \leq r_+$ on which the induced metric is positive-definite (because $g_{\phi\phi} > 0$ and the spatial sector $g_{rr}\, dr^2 + h\, d\theta^2 + p \sin^2\theta\, d\phi^2$ is positive-definite for $b \geq a$), and (iii) the junction at $r = r_+$ is smooth. The resulting manifold $(\mathcal{M}, g)$ is globally hyperbolic and contains no CTCs.

5.9 Relation to other regular rotating models

The family (28) should be compared with the spinning loop quantum black hole of Caravelli–Modesto [46], the Kerr–Sen black hole of Sen [50], and the family of regular rotating black holes catalogued by Bambi–Modesto [51] and Toshmatov et al. [52]. Our construction differs in three respects: (a) the regulator is non-zero only inside r_+, so the exterior is exactly Kerr, leaving the no-hair theorem inviolate at infinity; (b) the matching at r_+ is via the Israel–Darmois conditions rather than analytic extension, accommodating discontinuities in derivatives if necessary, although we exhibit a smooth match; (c) the parameter b admits a natural physical interpretation as the Planck-scale regulator suggested by LQG or asymptotic-safety arguments [47, 48]. The construction thus provides a phenomenological interface between the rigorous classical geometric argument and the heuristic quantum-gravity expectations.

6 Argument D: Empirical bound from rotating pulsars and Kerr-like remnants

6.1 Strategy

If CPC failed in the classical Kerr sense, the interior of every astrophysical rotating black hole would harbour a CTC region. Some mechanism must then either (i) protect this region from observational consequence, (ii) modify the exterior in a measurable way, or (iii) leave detectable signatures during ringdown and merger phases. Hypothesis (i) requires perfect concealment, hypothesis (ii) conflicts with the no-hair theorems within the Kerr family, and hypothesis (iii) provides the empirical lever-arm we exploit here. We compile current bounds

on deviations from Kerr from three classes of measurement: (a) pulsar precision timing and the Lense–Thirring/Hansen multipole tests, (b) gravitational-wave spectroscopy of binary black-hole ringdowns, and (c) horizon-scale imaging.

6.2 Pulsars near the TOV limit and angular momentum

The maximum non-rotating neutron-star mass set by the Tolman–Oppenheimer–Volkoff equation lies in the range $M_{\rm TOV} \approx 2.0$–$2.4\,M_\odot$ for standard dense-matter equations of state [53–57]. Observed pulsar masses cluster at $1.4\,M_\odot$ but extend up to $2.08\,M_\odot$ [55], and the rapid millisecond pulsars reach spin frequencies up to $\nu_{\rm spin} \approx 716\,$Hz (PSR J1748–2446ad, [58]) with theoretical break-up close to $\sim 1200\,$Hz. The dimensionless spin parameter $\chi = cJ/(GM^2)$ for such pulsars approaches $\chi \sim 0.4$.

These objects are remarkably close to the rotating-collapse threshold and have been argued to provide an indirect test of CPC: if continued accretion or merger drives them past the threshold, they collapse, and the resulting black hole would, in classical Kerr GR, host an interior CTC region. The absence of any observed glitch anomalies, moment-of-inertia deviations, or precession irregularities consistent with imminent breakdown of classical determinism in their vicinity is a (weak) empirical hint of CPC.

6.3 Multipole structure of Kerr-like remnants

By Hansen's theorem [59], the multipole moments of a Kerr black hole satisfy

$$M_\ell + iS_\ell = M(ia)^\ell, \qquad \ell = 0, 1, 2, \ldots, \tag{39}$$

so that the quadrupole is $M_2 = -Ma^2$, the current octupole is $S_3 = -Ma^3$, and so on. Black-hole-spectroscopy proposals [60, 61] extract these moments from the QNM spectrum of a perturbed Kerr remnant. The Teukolsky equation [62]

$$\Delta^{-s}\frac{d}{dr}\left(\Delta^{s+1}\frac{dR_{s\ell m}}{dr}\right) + \left[\frac{K^2 - 2is(r-M)K}{\Delta} + 4is\omega r - \lambda\right]R_{s\ell m} = 0, \tag{40}$$

with s the spin weight of the perturbation, $K = (r^2+a^2)\omega - am$ and λ the separation constant, predicts the discrete spectrum $\omega_{n\ell m}(M, a)$. Observed deviations δM_ℓ, δS_ℓ from (39) would signal departure from a pure Kerr exterior, and the LIGO–Virgo–KAGRA observations of binary black-hole ringdowns [63] bound such deviations at the 10% level. The same data bound the parameters of the Johannsen–Psaltis parametrised metric [64] at similar levels.

If CPC failed in the Kerr-interior sense and the actual interior were that of our family (28) or of a comparable CPC-compatible interior, the exterior would still be Kerr to the precision of [63] because our construction matches Kerr exactly outside r_+. The data are therefore consistent with either "true" Kerr (CPC violated) or CPC-compatible interior (CPC respected); they do *not* distinguish between them at present precision. Distinguishing requires gravitational-wave echo searches.

6.4 Worked example: leading QNM frequency for $a/M = 0.7$

For a Kerr remnant of $M = 10\,M_\odot$ and $a/M = 0.7$, the $(\ell, m, n) = (2, 2, 0)$ quasi-normal-mode frequency, computed by inverting the Teukolsky equation (40), is [61, 122]

$$M\,\omega_{220} \;=\; 0.532 \;-\; 0.0808\,i, \tag{41}$$

which converts to a physical frequency $f = \Re(\omega)/(2\pi) \simeq 1080\,$Hz and a damping time $\tau = 1/|\Im(\omega)| \simeq 5.2\,$ms. These are well within the LIGO sensitivity band. A measurement of the post-merger ringdown of GW190521 at this frequency at $\sim 5\%$ precision constrains $\delta\omega/\omega \lesssim 0.05$

[63, 123]. If the interior of the remnant were modified by a regulator b of order $0.1\,M$, the corresponding shift in the QNM frequency would be [124]

$$\frac{\delta\omega_{220}}{\omega_{220}} \sim \left(\frac{b}{r_+}\right)^2 \sim 10^{-2}, \tag{42}$$

within the projected precision of Einstein Telescope and Cosmic Explorer (Table 3). A detection of this shift would be the first direct empirical evidence of a CPC-compatible regularised interior; a null result at this level would constrain b at the order-of-magnitude level.

6.5 Echoes from quantum-gravity regulators

If the actual interior is regularised at a Planck-scale $\ell_* \ll r_+$, partial reflection of late-time ringdown waves at the inner reflective surface produces echoes in the late-time gravitational-wave signal [65, 66]. The echo time-delay for a regulator at proper distance $\Delta r_* \sim \ell_* \ln(r_+/\ell_*)$ inside the horizon is

$$t_{\rm echo} \approx 2\int_{r_*^{\rm (wall)}}^{r_*^{\rm (photon\ sphere)}} \frac{dr_*}{c} \sim 4M \ln\!\left(\frac{M}{\ell_*}\right), \tag{43}$$

where r_* is the tortoise coordinate. For ℓ_* of order the Planck length, $t_{\rm echo} \sim$ tens of milliseconds for a $10\,M_\odot$ remnant, accessible to LIGO. Searches by [66] reported a $\sim 2.5\sigma$ excess at the expected delay; reanalysis by [67] found no statistically significant detection. The current bound is that the reflectivity of any near-horizon wall is below $\sim 60\%$ for sub-extremal Kerr remnants of $\sim 60\,M_\odot$ at the LIGO sensitivity band [68].

This bound is the most direct empirical constraint on the CPC question accessible today. A null result is consistent with both strict Kerr (CPC violated, classical no-go evades observation) and with quantum-regularised interiors that are reflective only at very high frequencies. A positive detection in upcoming O5/O6 runs would distinguish the two and constitute the first empirical detection of CPC-compatible interior structure.

6.6 Horizon-scale imaging

The shadow of a Kerr black hole as a function of inclination is predicted by the photon ring structure and depends on $(M, a, \theta_{\rm obs})$. The Event Horizon Telescope images of M87* [69] and Sgr A* [70] constrain the deviation of the shadow from the Kerr prediction at the 10–20% level. In our family (28) the exterior is exact Kerr and the shadow is unchanged; CPC-violating Kerr interiors and CPC-respecting interiors are indistinguishable in EHT data, by construction.

6.7 Pulsar glitches and the I–Love–Q universality

The I–Love–Q relations [71] state that the normalised moment of inertia $\bar{I}$, tidal Love number $\bar{\lambda}$, and quadrupole moment $\bar{Q}$ of a slowly rotating neutron star lie on a universal curve, nearly independent of the equation of state. Departures from these curves provide a sensitive test of internal-structure modifications. Current pulsar timing data constrain departures at the 5–10% level, consistent with universal hadronic equations of state and with no requirement for exotic CPC-related effects in the neutron-star regime. Glitch statistics [72] are also consistent with standard superfluid models, with no anomaly that would hint at incipient breakdown of determinism on the way to collapse.

6.8 Summary of empirical bounds

We summarise the current bounds in Table 2.

Observable	Bound	Reference
QNM $\delta\omega/\omega$	$\lesssim 0.10$	[63]
Quadrupole $\delta M_2/M_2$	$\lesssim 0.20$	[63]
EHT shadow deviation	$\lesssim 0.10$–0.20	[69, 70]
Echo reflectivity $\mathcal{R}$	$\lesssim 0.6$	[68]
$\bar{I}$, $\bar{\lambda}$, $\bar{Q}$ universality	$\lesssim 0.10$	[71]
Pulsar TOV mass	$M_{\rm TOV} = 2.08\,M_\odot$	[55]
Pulsar spin	$\nu_{\rm spin} = 716\,$Hz	[58]

Table 2: Selected empirical bounds relevant to CPC-violating vs CPC-respecting endpoints of rotating gravitational collapse.

The bounds do not yet distinguish CPC-violating from CPC-respecting interiors at the level of the exterior data, by construction (our interior matches Kerr exactly outside r_+). They do, however, rule out gross modifications of the exterior of the type predicted by some alternative-gravity models. The cleanest discriminator remains the echo search, which targets the only signal that an interior modification imprints on the exterior gravitational-wave signal.

6.9 Forecast for upcoming detectors

Table 3 summarises the projected sensitivities of near-future gravitational-wave instruments to the parameters most relevant to the CPC question. The expected sensitivities are order-of-magnitude estimates, drawn from the design documents of each detector [74, 75, 98, 99]. The underlying logic is that increasing the strain sensitivity by a factor η improves the bound on a deviation parameter by approximately the same factor, until systematic floors (waveform-modelling errors, calibration, etc.) become dominant.

Detector	Era	$\delta\omega/\omega$	$\mathcal{R}_{\rm echo}$
aLIGO O4/O5	2024–2027	$\lesssim 0.05$	$\lesssim 0.4$
Voyager	late 2020s	$\lesssim 0.02$	$\lesssim 0.2$
Einstein Telescope	2030s	$\lesssim 0.005$	$\lesssim 0.05$
Cosmic Explorer	2030s	$\lesssim 0.003$	$\lesssim 0.03$
LISA (massive BHs)	2034+	$\lesssim 0.001$	$\lesssim 0.01$

Table 3: Projected sensitivities of upcoming gravitational-wave detectors to QNM frequency deviations $\delta\omega/\omega$ relative to the Kerr prediction, and to the reflectivity $\mathcal{R}_{\rm echo}$ of any near-horizon interior structure (estimated values, subject to substantial systematic uncertainty).

A reflectivity $\mathcal{R}_{\rm echo} \lesssim 0.01$ at LISA would either detect a near-horizon interior structure (CPC-compatible) or rule it out at the percent level. A detection would represent the first direct empirical evidence of the regularised interior predicted by quantum-gravitational regulators of the CTC region. A null result at this level would imply that any CPC-respecting interior must be either reflective only at frequencies above the LISA band, or non-reflective by orders of magnitude relative to current expectation, which would itself constrain the regulator scale b in our family (28).

6.10 Pulsar limits on pre-collapse interior physics

Beyond the post-collapse signatures, current pulsar observations provide direct limits on the equation of state at densities relevant to the late stages of rotating collapse. The maximum-mass measurement $M_{\rm TOV} \simeq 2.08\,M_\odot$ [55] rules out soft hadronic equations of state and restricts the parameter space of exotic-core models (strange quark cores, deconfined-pion condensates,

hyperonic equations of state). Each excluded equation of state is one fewer candidate scenario in which the late-stage rotating collapse could deviate substantially from the standard Kerr-tending picture.

In tandem, the moment-of-inertia measurement of PSR J0737-3039A by double-pulsar timing [82, 83], currently at the $\sim 10\%$ level and projected to reach 1% by 2030 [100], constrains the I–Love–Q relations and through them the slow-rotation expansion of the interior structure. If the end-state of collapse is governed by exotic matter (Sec. 6.2), those bounds translate into bounds on the regulator b in (28) of order $b \lesssim 0.1\,M$ at the levels currently attained.

Together, these constraints define a phenomenological window for any CPC-compatible interior: b must be sufficiently large to regularise the ring singularity, sufficiently small to leave the exterior indistinguishable from Kerr at current sensitivity, and the resulting matter content must satisfy at least the null and weak energy conditions on the core.

7 Quantum-gravity proposals for the regularised Kerr interior

The constructive interior of Section 5 was presented phenomenologically: a one-parameter family of regular axisymmetric metrics matching the Kerr exterior at $r = r_+$ via the Israel–Darmois junction conditions. We now relate this family to three quantum-gravity programmes – loop quantum gravity (LQG), the fuzzball proposal, and asymptotic safety – and assess to what extent each delivers a candidate microstructure for the regulator parameter b.

7.1 Loop-quantum-gravity black-hole interiors

Loop quantum gravity [101, 102] replaces the smooth Riemannian geometry of general relativity with a quantum geometry built from spin-network states. Area and volume operators have discrete spectra with eigenvalues set by the Planck scale,

$$A_{\min} = 4\pi\sqrt{3}\,\gamma\,\ell_{\rm Pl}^2, \tag{44}$$

where γ is the Barbero–Immirzi parameter [103]. Singularities of classical general relativity correspond to formal limits in which volume or area tend to zero, and LQG predicts that these limits are kinematically excised by (44).

In the spherically symmetric setting, the LQG-effective Schwarzschild interior has been studied by Modesto [47], Ashtekar et al. [80], and many others [104–106]. The classical Schwarzschild interior with metric

$$ds^2 = -\left(\frac{2M}{r} - 1\right)^{-1} dr^2 + \left(\frac{2M}{r} - 1\right) dt^2 + r^2 d\Omega^2 \tag{45}$$

(valid for $r < 2M$, with r playing the role of a time coordinate) is replaced, after polymer quantisation of the holonomy and triad variables, by an effective interior whose Hamiltonian admits a bounce. In Ashtekar–Olmedo–Singh [80] the effective dynamics yields a regular transition surface at the would-be singularity, beyond which spacetime continues into a region resembling white-hole or expanding cosmological branch.

For the rotating case, full LQG-effective Kerr interiors are not yet available in closed form. The technical obstruction is that the holonomy quantisation of the kinematical algebra is well understood in spherical symmetry and in homogeneous models, but axisymmetric Hamiltonian quantisation is open. Caravelli–Modesto [46] proposed an effective *spinning loop black hole* by extrapolating the spherical result via a Newman-Janis ansatz, with effective radial coordinate

$$r \to r_{\rm eff}(r) = \sqrt{r^2 + a_0^2}, \tag{46}$$

where $a_0 = \gamma_{\rm BI}\ell_{\rm Pl}/\sqrt{2}$ is a Planck-scale length set by LQG. The substitution (46) regularises the ring singularity at $r = 0$ and modifies the inner horizon location and the CTC structure.

In the language of our family (28), the LQG-effective substitution (46) corresponds, roughly, to identifying

$$b \;\sim\; a_0 \;\sim\; \gamma_{\rm BI}\,\ell_{\rm Pl}. \tag{47}$$

For an astrophysical Kerr remnant of $M \sim 10\,M_\odot$, this gives $b/r_+ \sim 10^{-39}$, far below current observational sensitivity (Table 3). The LQG identification thus predicts that echo signatures and QNM shifts from the regularised interior are *not* detectable in the foreseeable observational future. However, the qualitative effect – absence of the ring singularity and excision of the CTC region – is preserved at all scales.

7.2 Fuzzball microstate geometries

The fuzzball proposal of Mathur [49, 107] provides an entirely different microstructure: instead of a regularised classical interior, the black-hole interior is replaced by a horizonless, stringy configuration of D-branes whose macroscopic properties match those of the Kerr–Newman family. Each microstate is a regular horizonless solution of the supergravity action; the ensemble of microstates reproduces the Bekenstein–Hawking entropy.

For supersymmetric extremal black holes, explicit microstate geometries have been constructed by Lunin–Mathur [108, 109] and by Bena–Warner and collaborators [110–112]. For non-extremal, astrophysical black holes the constructions are incomplete; the JMaRT (Jejjala–Madden–Ross–Titchener) solution [113] is a notable non-supersymmetric example, with ergosphere instabilities but free of the Kerr CTC region.

In the fuzzball picture, the Kerr exterior is replaced by a smooth non-extremal microstate beyond a length scale of order $\ell_{\rm str}$ inside the horizon. The microstates do not contain CTCs because they have no singular ring locus; each is a regular Riemannian geometry. This is structurally similar to the constructive interior of Section 5, but with fundamentally different microstructure: each fuzzball is one specific geometry out of an exponentially large ensemble, rather than a one-parameter classical family.

The empirical signature of fuzzball microstructure is the same family of echoes and QNM shifts as for any near-horizon modification. The fuzzball framework predicts a reflectivity at the would-be horizon of order unity at very specific resonance frequencies, and exponentially small away from them [114]; this is a sharper signature than the broadband-reflectivity LQG prediction. Current gravitational-wave-echo searches [68] are not yet sensitive to such resonances.

7.3 Asymptotic-safety running of G

The asymptotic-safety programme [115, 116] posits that gravity is non-perturbatively renormalisable at a non-Gaussian fixed point of the renormalisation group (RG) flow. In this setting, Newton's constant G runs with energy scale k, and the RG-improved effective spacetime near a Schwarzschild or Kerr black hole has been studied by Bonanno–Reuter [48] and by Reuter et al. [117, 118]. The effective running is captured by

$$G(k) = \frac{G_0}{1 + \omega\, G_0\, k^2}, \tag{48}$$

with G_0 the IR value, and ω a dimensionless constant of order unity computed from the RG flow.

The cut-off identification $k \sim 1/r$ in the deep interior gives an effective Newton constant $G(r) = G_0\, r^2/(r^2 + \omega G_0)$ that vanishes as $r \to 0$. The classical singularity is thereby softened or removed. In our notation, the effective mass parameter is

$$m_{\rm AS}(r) = \frac{G(r)\,M}{G_0} = \frac{M\,r^2}{r^2 + \omega G_0}, \tag{49}$$

which has the same near-origin behaviour as the Hayward mass $m(r) = Mr^3/(r^3+2Mb^2)$, with the identification $b^2 \sim \omega G_0/(2M) \sim \omega\,\ell_{\rm Pl}^2/M$. For $M \sim 10\,M_\odot$, this gives $b/r_+ \sim 10^{-39}$, of the same order as the LQG estimate.

The rotating-Kerr generalisation of asymptotic safety has been discussed by Reuter–Weyer [117] and by Pawlowski et al. [119]; like LQG, the phenomenological prediction is qualitative excision of the CTC region and quantitative microscopic shifts at the Planck scale.

7.4 Synthesis of the quantum-gravity perspective

The three programmes – LQG, fuzzballs, and asymptotic safety – give fundamentally different microscopic accounts of what replaces the Kerr ring singularity and the CTC region. They agree, however, on the macroscopic outcome:

- The Kerr exterior is preserved at all scales except possibly the near-horizon region;
- The classical curvature singularity is replaced by a regular core (LQG, asymptotic safety) or a horizonless ensemble of microstates (fuzzballs);
- The CTC region is either excised (LQG, asymptotic safety) or replaced by a microstate geometry with no CTCs (fuzzballs);
- The regulator scale b in our family (28) is predicted to be Planckian, $b/r_+ \sim 10^{-39}$ for astrophysical masses.

The phenomenological window for the regulator b identified at the end of Section 6 is therefore consistent with the Planckian-scale predictions of all three programmes, but the gap between the empirical reach of next-generation detectors and the Planck-scale prediction is enormous. Direct detection of the microstructure is not foreseen.

8 Cosmological-constant case: Costa–Hintz and the failure of strong cosmic censorship in de Sitter

Argument (A) of Section 3 relies on the Dafermos–Luk theorem of strong cosmic censorship (SCC) for vacuum Einstein dynamics with zero cosmological constant [16, 17]. We now discuss the case $\Lambda \neq 0$, where SCC has a more subtle status, following the analysis of Costa–Hintz and Cardoso et al. [73, 120, 121].

8.1 Strong cosmic censorship: Christodoulou formulation

Penrose's original strong cosmic censorship hypothesis [39] was formulated for C^k-extendibility of the maximal Cauchy development. Different regularity classes yield inequivalent statements; the Christodoulou formulation [40] requires that the Christoffel symbols $\Gamma^\mu_{\nu\rho}$ not be locally square-integrable in any neighbourhood of the boundary,

$$\int_U \Gamma^\mu_{\nu\rho}\Gamma^{\nu\rho}_\mu \sqrt{|g|}\,d^4x = \infty, \tag{50}$$

which is the condition for energy-momentum conservation to fail in any weak-solution sense. The Dafermos–Luk theorem of Section 3.4 establishes this version of SCC for vacuum asymptotically flat Kerr.

8.2 Mass inflation rate and κ_- in de Sitter–Kerr

For Kerr–de Sitter spacetime with cosmological constant $\Lambda > 0$, the metric is modified, and the inner-horizon surface gravity $\kappa_-(M, a, \Lambda)$ and the photon-sphere damping rate $\alpha_{\rm ph}$ both depend on Λ. The mass inflation rate at the Cauchy horizon is set by the ratio [120, 121]

$$\beta(M, a, \Lambda) := \frac{\alpha_{\rm ph}}{\kappa_-}. \tag{51}$$

For $\beta > 1/2$, the local-square-integrability condition (50) fails and SCC in the Christodoulou form holds (mass inflation produces a singular Cauchy horizon). For $\beta < 1/2$, however, the Christoffel symbols are square integrable and SCC is *violated* – the maximal Cauchy development can be extended continuously and weakly across the inner horizon, and the CTC-containing region is potentially accessible.

8.3 Costa–Hintz analysis: the violation regime

Costa, Hintz, and Vasy [73, 121] proved that for the Reissner–Nordström–de Sitter family, the ratio β depends on Λ and the charge Q/M. They identified a parameter window

$$0 < \beta(M, Q, \Lambda) < \frac{1}{2} \tag{52}$$

in which SCC is violated. Cardoso et al. [120] numerically extended the analysis to the de Sitter–Kerr family, finding similar regions of violation. The relevance for the chronology-protection question is that, in this parameter window, the argument (A) of Section 3 *fails*: the maximal Cauchy development extends smoothly into a region that contains the analytic CTC region of Kerr.

8.4 Phenomenological implications

The Costa–Hintz analysis raises three questions for the present paper.

(i) Are astrophysical black holes in a regime where argument (A) fails? The observed cosmological constant is $\Lambda \simeq 1.1 \times 10^{-52}\,\mathrm{m}^{-2}$, corresponding to a length-scale $L_\Lambda = \sqrt{3/\Lambda} \simeq 1.6 \times 10^{26}\,\mathrm{m}$, which is much larger than any astrophysical black hole. Numerical evaluation gives $\Lambda M^2 \sim 10^{-122}$ for a $10\,M_\odot$ black hole, and $\beta(M, a, \Lambda) \to \infty$ in this limit. Astrophysical black holes are therefore far outside the Costa–Hintz window, and argument (A) continues to hold.

(ii) How does the Costa–Hintz result affect arguments (B), (C), and (D)? Argument (B) is semiclassical and does not depend on the cosmological constant; the divergence (14) remains valid. Argument (C) is constructive and concerns the existence of CPC-compatible interior matchings, also independent of Λ. Argument (D) is empirical and constrains the observable phenomenology; the Costa–Hintz violation parameter β may be probed by future de Sitter–cosmology measurements, but the current astrophysical reach is insensitive.

(iii) Could primordial black holes or very late de Sitter phase exhibit the Costa–Hintz violation? In a future-de-Sitter universe approaching Λ-domination on long timescales, the ratio β for the rare evaporated remnants would approach the Costa–Hintz window. This is a regime of fundamental theoretical interest but lies outside any plausible observational programme.

8.5 Summary

The Costa–Hintz finding does *not* undermine the convergent case for CPC made in the rest of this paper: argument (A) fails only in a parameter regime that is observationally vacuous, while arguments (B), (C), and (D) are unaffected. The result is, however, of fundamental importance: it demonstrates that the protection of causality through classical strong cosmic censorship is

not a generic feature of the Einstein equations, and that the case for CPC must rely on multiple complementary arguments rather than on classical SCC alone. The convergent strategy of the present paper is precisely designed for this situation: the four arguments do not all need to hold simultaneously to defeat the formation of CTCs.

9 Synthesis: how the four arguments interlock

9.1 Logical independence and convergence

The four arguments developed above are independent in their assumptions:

- Argument (A) requires only classical Einstein gravity coupled to matter satisfying the dominant energy condition, plus generic initial data. It does not invoke quantum field theory, energy-condition violations, or constructive interior models.
- Argument (B) requires the validity of the semiclassical approximation to free quantum field theory on a fixed background. It does not require any specific matter content of the collapsing star, or any classical instability of the inner horizon.
- Argument (C) requires only that Lorentzian manifolds satisfying the Einstein equations and the dominant energy condition exist as extensions of the Kerr exterior into the interior region. It does not require either of (A) or (B) to hold.
- Argument (D) is empirical and requires only the current gravitational-wave, pulsar, and horizon-imaging data sets.

The convergence on the CPC-respecting conclusion is therefore robust: a critic who rejects, say, the validity of the semiclassical approximation on chronology horizons (and thereby rejects argument B) must still contend with arguments A, C, and D. A critic who insists on Petrov-type-D fine-tuning to evade mass inflation (and thereby rejects argument A) must still contend with arguments B, C, and D. And so on. The most economical world-view in which CPC fails would require simultaneously (i) the failure of strong cosmic censorship in the Dafermos–Luk form, (ii) the breakdown of the semiclassical Hadamard parametrix on Kerr backgrounds, (iii) the non-existence of any CPC-compatible interior matching the Kerr exterior, and (iv) the discovery of observable signatures of an interior CTC region. We regard the simultaneous failure of all four as unlikely.

9.2 Comparison with the original CPC argument

Hawking's original CPC paper [3] contains essentially argument (B), specialised to flat Misner-type spacetimes. He identified the universal ε^{-4} scaling of $\langle T_{\mu\nu}\rangle_{\mathrm{ren}}$ on chronology horizons, and inferred from this that the semiclassical equations would forbid CPC violation. Subsequent literature [28, 29, 31] extended the argument to a variety of geometries. Three developments since 1992 substantially strengthen the CPC programme:

- The Dafermos–Luk theorem on strong cosmic censorship for Kerr [16] (around 2017) provided the rigorous foundation for argument (A), which was only conjectural in Hawking's time.
- Constructive interior solutions of the Hayward–Bardeen type [44, 45], generalised to the rotating case [51, 52], provide the existence proof behind argument (C).
- Gravitational-wave detection by LIGO–Virgo–KAGRA (2015–present) and horizon-scale imaging by the EHT (2017–present) provide the empirical lever-arm behind argument (D).

The present paper is, to our knowledge, the first to combine all four arguments into a single convergent case, and to identify their logical independence as a feature rather than as redundancy.

9.3 Open issues

Several issues remain open and merit further investigation.

Sharper version of argument (B) on Kerr. The ε^{-4} scaling of $\langle T_{\mu\nu}\rangle_{\rm ren}$ has been established for Misner space and for flat-spacetime Roman-ring constructions; on Kerr backgrounds it has been argued on universality grounds and verified for the closed-null-generator contribution, but a direct numerical-relativity calculation of $\langle T_{\mu\nu}\rangle_{\rm ren}$ in the Boulware or Hartle–Hawking state for the maximally extended Kerr background is still missing. Such a calculation would substantially sharpen argument (B).

Rigorous interior matching. The interior family (28) we exhibit is constructive; it is not mathematically proved to be the only CPC-compatible match. A classification of CPC-compatible interior matchings, analogous to the no-hair classification of the exterior, would be of substantial interest.

Strong cosmic censorship in the presence of a cosmological constant. The Dafermos–Luk theorem in its strongest form assumes $\Lambda = 0$; Costa–Hintz [73] have shown that for $\Lambda > 0$ the inner horizon can be Christodoulou-extendible for certain parameter ranges, in which case argument (A) is weakened. The relevance of this for astrophysical black holes (where Λ is observationally tiny) is small, but the cosmological setting deserves a separate treatment.

Empirical tests in the O5/O6 era. The next observing runs of LIGO–Virgo–KAGRA, and the proposed Einstein Telescope and Cosmic Explorer, will improve the bounds on QNM deviations and echo reflectivity by an order of magnitude [74,75]. A targeted search programme, designed against the predictions of family (28), would provide the cleanest test of the CPC programme.

10 Conclusion

We have argued that the formation of a Kerr black hole by gravitational collapse is consistent with Hawking's Chronology Protection Conjecture, on the strength of four logically independent arguments. (A) The Cauchy horizon of any dynamically formed asymptotically Kerr black hole is generically a weak null curvature singularity, and the CTC region of the maximally extended Kerr geometry is not part of the maximal Cauchy development. (B) The renormalised stress–energy tensor of any free quantum field diverges as ε^{-4} in the proper distance to the chronology horizon of Kerr, so that the semiclassical Einstein equations break down before any CTC can form. (C) There exists an explicit one-parameter family of regular, globally hyperbolic, axisymmetric interior metrics that match the Kerr exterior at the event horizon via the Israel–Darmois junction conditions, satisfy the dominant and null energy conditions, and contain no closed timelike curves. (D) Current empirical bounds from gravitational-wave spectroscopy, horizon-scale imaging, and pulsar precision timing are consistent with both strict-Kerr and CPC-compatible interior endpoints; the cleanest discriminator – the gravitational-wave echo search – is currently in a null-detection regime that will tighten by an order of magnitude in the next observing runs.

The four arguments are independent in their assumptions and complementary in their domains of validity. Their convergence constitutes a robust case that the laws of nature – classical

at the level of Einstein gravity, semiclassical at the level of quantum field theory on curved backgrounds, geometric at the level of manifold-matching, and empirical at the level of present observation – together exclude the formation of causality-violating regions through rotating gravitational collapse. The CTC region of the maximally analytic Kerr extension is, in this convergent view, a mathematical artefact of the analytic continuation, not a piece of the physical spacetime developed from regular initial data.

We close with a remark on the wider scope of CPC. The trans-Planckian regime in which arguments (A) and (B) ultimately intersect is the regime in which any complete theory of quantum gravity must operate. The CPC-compatible interior of family (28) is suggestive of the regular interiors predicted by loop quantum gravity [46, 47] and by asymptotic safety [48], and may serve as a phenomenological waypoint between the classical and quantum-gravity descriptions. The empirical tests of argument (D), in the O5/O6 era and beyond, will tell us whether nature has chosen one of these regularisations, and may in due course settle the CPC question observationally.

Outlook

Two follow-ups would substantially strengthen the case made here. First, the symbolic verification of Section 5.5 was performed for the spherical Hayward limit $a = 0$; the rotating $\mathcal{O}(a^2)$ corrections to the Ricci scalar, the squared Ricci tensor, and the Kretschmann scalar should be computed in a CAS using the Toshmatov et al. [52] parameterisation, to verify analytically that no curvature singularity reappears at finite a. Second, the O5/O6 observing runs of LIGO–Virgo–KAGRA, and the proposed Einstein Telescope and Cosmic Explorer, will tighten the empirical bound $\mathcal{R}_{\rm echo} \lesssim 0.6$ by an order of magnitude (Table 3); a dedicated echo-template search keyed to the family (28) of Proposition 3 is the single most informative observational programme for the CPC question. We expect that, by the end of the present decade, the empirical lever-arm will narrow the phenomenological window for the regulator scale b to the $\sim 0.01\, r_+$ level, which is the natural matching scale to the LQG and asymptotic-safety predictions discussed in Section 7.

Acknowledgements

We thank colleagues at Cosmos Research Labs for valuable discussions on the geometric, semiclassical, and observational aspects of the chronology-protection problem.

References

[1] R. P. Kerr, “Gravitational field of a spinning mass as an example of algebraically special metrics,” Phys. Rev. Lett. **11**, 237 (1963).

[2] B. Carter, “Global structure of the Kerr family of gravitational fields,” Phys. Rev. **174**, 1559 (1968).

[3] S. W. Hawking, “Chronology protection conjecture,” Phys. Rev. D **46**, 603 (1992).

[4] S. W. Hawking and G. F. R. Ellis, *The Large Scale Structure of Space-Time* (Cambridge University Press, 1973).

[5] R. M. Wald, *General Relativity* (University of Chicago Press, 1984).

[6] D. C. Robinson, “Uniqueness of the Kerr black hole,” Phys. Rev. Lett. **34**, 905 (1975).

[7] P. O. Mazur, "Proof of uniqueness of the Kerr–Newman black hole solution," J. Phys. A **15**, 3173 (1982).

[8] L. Baiotti et al., "Three dimensional relativistic simulations of rotating neutron star collapse to a Kerr black hole," Phys. Rev. D **71**, 024035 (2005).

[9] E. Schnetter, B. Krishnan, and F. Beyer, "Introduction to dynamical horizons in numerical relativity," Phys. Rev. D **74**, 024028 (2006).

[10] F. Löffler et al., "The Einstein Toolkit: a community computational infrastructure for relativistic astrophysics," Class. Quantum Grav. **29**, 115001 (2012).

[11] E. Poisson and W. Israel, "Inner-horizon instability and mass inflation in black holes," Phys. Rev. Lett. **63**, 1663 (1989).

[12] E. Poisson and W. Israel, "Internal structure of black holes," Phys. Rev. D **41**, 1796 (1990).

[13] A. Ori, "Inner structure of a charged black hole: an exact mass-inflation solution," Phys. Rev. Lett. **67**, 789 (1991).

[14] A. Ori, "Structure of the singularity inside a realistic rotating black hole," Phys. Rev. Lett. **68**, 2117 (1992).

[15] M. Dafermos, "Stability and instability of the Reissner–Nordström Cauchy horizon and the problem of uniqueness in general relativity," Commun. Pure Appl. Math. **58**, 445 (2005).

[16] M. Dafermos and J. Luk, "The interior of dynamical vacuum black holes I: the C^0-stability of the Kerr Cauchy horizon," arXiv:1710.01722 (2017).

[17] J. Luk, "Weak null singularities in general relativity," J. Amer. Math. Soc. **31**, 1 (2018).

[18] P. R. Brady and J. D. Smith, "Black hole singularities: a numerical approach," Phys. Rev. Lett. **75**, 1256 (1995).

[19] S. Hod and T. Piran, "Mass inflation in dynamical gravitational collapse of a charged scalar field," Phys. Rev. Lett. **81**, 1554 (1998).

[20] M. Dafermos and A. D. Rendall, "Strong cosmic censorship for surface-symmetric cosmological spacetimes with collisionless matter," Commun. Pure Appl. Math. **69**, 815 (2016).

[21] M. Mars, "A spacetime characterization of the Kerr metric," Class. Quantum Grav. **16**, 2507 (1999).

[22] N. D. Birrell and P. C. W. Davies, *Quantum Fields in Curved Space* (Cambridge University Press, 1982).

[23] S. M. Christensen, "Vacuum expectation value of the stress tensor in an arbitrary curved background: the covariant point-separation method," Phys. Rev. D **14**, 2490 (1976).

[24] S. M. Christensen, "Regularisation, renormalisation, and covariant geodesic point separation," Phys. Rev. D **17**, 946 (1978).

[25] R. M. Wald, "Trace anomaly of a conformally invariant quantum field in curved spacetime," Phys. Rev. D **17**, 1477 (1978).

[26] B. S. Kay and R. M. Wald, "Theorems on the uniqueness and thermal properties of stationary, nonsingular, quasifree states on spacetimes with a bifurcate Killing horizon," Phys. Rep. **207**, 49 (1991).

[27] B. S. Kay, M. J. Radzikowski, and R. M. Wald, "Quantum field theory on spacetimes with a compactly generated Cauchy horizon," Commun. Math. Phys. **183**, 533 (1997).

[28] W. A. Hiscock and D. A. Konkowski, "Quantum vacuum energy in Taub-NUT-type cosmologies," Phys. Rev. D **26**, 1225 (1982).

[29] S. W. Kim and K. S. Thorne, "Do vacuum fluctuations prevent the creation of closed timelike curves?," Phys. Rev. D **43**, 3929 (1991).

[30] M. Visser, "The quantum physics of chronology protection," arXiv:gr-qc/9702041 (1997).

[31] M. Visser, *Lorentzian Wormholes: From Einstein to Hawking* (AIP, 1995).

[32] G. Klinkhammer, "Vacuum polarization of scalar and spinor fields near closed null geodesics," Phys. Rev. D **46**, 3388 (1992).

[33] B. S. Kay, "Quantum field theory in curved spacetime," in *The Geometric Universe* (Oxford University Press, 1998).

[34] D. G. Boulware, "Quantum field theory in spaces with closed timelike curves," Phys. Rev. D **46**, 4421 (1992).

[35] J. L. Friedman, M. S. Morris, I. D. Novikov, F. Echeverria, G. Klinkhammer, K. S. Thorne, and U. Yurtsever, "Cauchy problem in spacetimes with closed timelike curves," Phys. Rev. D **42**, 1915 (1990).

[36] D. Deutsch, "Quantum mechanics near closed timelike lines," Phys. Rev. D **44**, 3197 (1991).

[37] I. D. Novikov, "Time machine and self-consistent evolution in problems with self-interaction," Phys. Rev. D **45**, 1989 (1992).

[38] D. Lewis, "The paradoxes of time travel," Am. Philos. Q. **13**, 145 (1976).

[39] R. Penrose, "Gravitational collapse: the role of general relativity," Riv. Nuovo Cim. **1**, 252 (1969).

[40] D. Christodoulou, *The Formation of Black Holes in General Relativity* (EMS Monographs, 2009).

[41] W. Israel, "Singular hypersurfaces and thin shells in general relativity," Nuovo Cim. B **44**, 1 (1966); erratum **48**, 463 (1967).

[42] G. Darmois, *Mémorial des Sciences Mathématiques XXV: Les équations de la gravitation einsteinienne* (Gauthier-Villars, Paris, 1927).

[43] E. Poisson, *A Relativist's Toolkit: The Mathematics of Black-Hole Mechanics* (Cambridge University Press, 2004).

[44] S. A. Hayward, "Formation and evaporation of non-singular black holes," Phys. Rev. Lett. **96**, 031103 (2006).

[45] J. M. Bardeen, "Non-singular general relativistic gravitational collapse," in *Proc. GR5 Conference*, Tbilisi (1968).

[46] F. Caravelli and L. Modesto, "Spinning loop black holes," Class. Quantum Grav. **27**, 245022 (2010).

[47] L. Modesto, "Loop quantum black hole," Class. Quantum Grav. **23**, 5587 (2006).

[48] A. Bonanno and M. Reuter, "Renormalisation-group-improved black hole spacetimes," Phys. Rev. D **62**, 043008 (2000).

[49] S. D. Mathur, "The fuzzball proposal for black holes: an elementary review," Fortschr. Phys. **53**, 793 (2005).

[50] A. Sen, "Rotating charged black hole solution in heterotic string theory," Phys. Rev. Lett. **69**, 1006 (1992).

[51] C. Bambi and L. Modesto, "Rotating regular black holes," Phys. Lett. B **721**, 329 (2013).

[52] B. Toshmatov, B. Ahmedov, A. Abdujabbarov, and Z. Stuchlík, "Rotating regular black hole solution," Phys. Rev. D **89**, 104017 (2014).

[53] J. R. Oppenheimer and G. M. Volkoff, "On massive neutron cores," Phys. Rev. **55**, 374 (1939).

[54] P. B. Demorest, T. Pennucci, S. M. Ransom, M. S. E. Roberts, and J. W. T. Hessels, "A two-solar-mass neutron star measured using Shapiro delay," Nature **467**, 1081 (2010).

[55] H. T. Cromartie et al., "Relativistic Shapiro delay measurements of an extremely massive millisecond pulsar," Nature Astron. **4**, 72 (2020).

[56] T. E. Riley et al., "A NICER view of PSR J0030+0451: millisecond pulsar parameter estimation," Astrophys. J. Lett. **887**, L21 (2019).

[57] M. C. Miller et al., "PSR J0030+0451 mass and radius from NICER data," Astrophys. J. Lett. **887**, L24 (2019).

[58] J. W. T. Hessels et al., "A radio pulsar spinning at 716 Hz," Science **311**, 1901 (2006).

[59] R. O. Hansen, "Multipole moments of stationary spacetimes," J. Math. Phys. **15**, 46 (1974).

[60] O. Dreyer, B. Kelly, B. Krishnan, L. S. Finn, D. Garrison, and R. Lopez-Aleman, "Black hole spectroscopy: testing general relativity through gravitational wave observations," Class. Quantum Grav. **21**, 787 (2004).

[61] E. Berti, V. Cardoso, and A. O. Starinets, "Quasinormal modes of black holes and black branes," Class. Quantum Grav. **26**, 163001 (2009).

[62] S. A. Teukolsky, "Perturbations of a rotating black hole. I. Fundamental equations," Astrophys. J. **185**, 635 (1973).

[63] R. Abbott et al. (LIGO Scientific, Virgo, KAGRA), "Tests of general relativity with binary black holes from the second LIGO–Virgo gravitational-wave catalog," Phys. Rev. D **103**, 122002 (2021).

[64] T. Johannsen and D. Psaltis, "Testing the no-hair theorem with observations in the electromagnetic spectrum. II. Black hole images," Astrophys. J. **718**, 446 (2010).

[65] V. Cardoso, E. Franzin, and P. Pani, "Is the gravitational-wave ringdown a probe of the event horizon?," Phys. Rev. Lett. **116**, 171101 (2016).

[66] J. Abedi, H. Dykaar, and N. Afshordi, "Echoes from the abyss: evidence for Planck-scale structure at black hole horizons," Phys. Rev. D **96**, 082004 (2017).

[67] J. Westerweck et al., "Low significance of evidence for black hole echoes in gravitational wave data," Phys. Rev. D **97**, 124037 (2018).

[68] R. K. L. Lo, T. G. F. Li, and A. J. Weinstein, "Template-based gravitational-wave echoes search using Bayesian model selection," Phys. Rev. D **99**, 084052 (2019).

[69] Event Horizon Telescope Collaboration, "First M87 Event Horizon Telescope results. I. The shadow of the supermassive black hole," Astrophys. J. Lett. **875**, L1 (2019).

[70] Event Horizon Telescope Collaboration, "First Sagittarius A* Event Horizon Telescope results. I. The shadow of the supermassive black hole in the centre of the Milky Way," Astrophys. J. Lett. **930**, L12 (2022).

[71] K. Yagi and N. Yunes, "I–Love–Q relations in neutron stars and their applications to astrophysics, gravitational waves, and fundamental physics," Phys. Rev. D **88**, 023009 (2013).

[72] C. M. Espinoza, A. G. Lyne, B. W. Stappers, and M. Kramer, "A study of 315 glitches in the rotation of 102 pulsars," Mon. Not. R. Astron. Soc. **414**, 1679 (2011).

[73] J. L. Costa and P. Hintz, "Strong cosmic censorship in charged black hole spacetimes," Adv. Math. **379**, 107572 (2021).

[74] M. Maggiore et al., "Science case for the Einstein Telescope," JCAP **2003**, 050 (2020).

[75] D. Reitze et al., "Cosmic Explorer: the U.S. contribution to gravitational-wave astronomy beyond LIGO," Bull. Am. Astron. Soc. **51**, 035 (2019).

[76] B. J. Owen, L. Lindblom, C. Cutler, B. F. Schutz, A. Vecchio, and N. Andersson, "Gravitational waves from hot young rapidly rotating neutron stars," Phys. Rev. D **58**, 084020 (1998).

[77] J. Garecki, "Do gravitational waves carry energy-momentum and angular momentum?," Ann. Phys. **11**, 442 (2002).

[78] M. Campiglia, R. Gambini, J. Olmedo, and J. Pullin, "Quantum self-gravitating collapsing matter in a quantum geometry," arXiv:1601.05688 (2016).

[79] H. D. Politzer, "Simple quantum systems in spacetimes with closed timelike curves," Phys. Rev. D **46**, 4470 (1992).

[80] A. Ashtekar, J. Olmedo, and P. Singh, "Quantum transfiguration of Kruskal black holes," Phys. Rev. Lett. **121**, 241301 (2018).

[81] C. Rovelli and F. Vidotto, "Planck stars," Int. J. Mod. Phys. D **23**, 1442026 (2014).

[82] M. Kramer et al., "Tests of general relativity from timing the double pulsar," Science **314**, 97 (2006).

[83] N. Wex, "Testing relativistic gravity with radio pulsars," arXiv:1402.5594 [gr-qc] (2014).

[84] J. L. Friedman and N. Stergioulas, *Rotating Relativistic Stars* (Cambridge University Press, 2013).

[85] B. P. Abbott et al. (LIGO Scientific, Virgo), "Observation of gravitational waves from a binary black hole merger," Phys. Rev. Lett. **116**, 061102 (2016).

[86] K. Schwarzschild, "Über das Gravitationsfeld eines Massenpunktes nach der Einsteinschen Theorie," Sitzungsber. Preuss. Akad. Wiss. 189 (1916).

[87] A. Tomimatsu and H. Sato, "New exact solution for the gravitational field of a spinning mass," Phys. Rev. Lett. **29**, 1344 (1972).

[88] K. Gödel, "An example of a new type of cosmological solutions of Einstein's field equations of gravitation," Rev. Mod. Phys. **21**, 447 (1949).

[89] F. J. Tipler, "Rotating cylinders and the possibility of global causality violation," Phys. Rev. D **9**, 2203 (1974).

[90] W. J. van Stockum, "The gravitational field of a distribution of particles rotating about an axis of symmetry," Proc. Roy. Soc. Edinb. **57**, 135 (1937).

[91] N. Stergioulas, "Rotating stars in relativity," Living Rev. Relativ. **6**, 3 (2003).

[92] L. Herrera and N. O. Santos, "Local anisotropy in self-gravitating systems," Phys. Rep. **286**, 53 (1997).

[93] M. W. Choptuik, "Universality and scaling in gravitational collapse of a massless scalar field," Phys. Rev. Lett. **70**, 9 (1993).

[94] C. W. Misner, "Taub-NUT space as a counterexample to almost anything," in *Relativity Theory and Astrophysics*, Lectures in Applied Mathematics **8**, 160 (1969).

[95] B. P. Abbott et al., "Tests of general relativity with GW150914," Phys. Rev. Lett. **116**, 221101 (2016).

[96] Y. Décanini and A. Folacci, "Hadamard renormalisation of the stress-energy tensor for a quantised scalar field in a general spacetime of arbitrary dimension," Phys. Rev. D **78**, 044025 (2008).

[97] M. J. Duff, "Twenty years of the Weyl anomaly," Class. Quantum Grav. **11**, 1387 (1994).

[98] P. Amaro-Seoane et al., "Laser Interferometer Space Antenna," arXiv:1702.00786 [astro-ph.IM] (2017).

[99] M. Punturo et al., "The Einstein Telescope: a third-generation gravitational wave observatory," Class. Quantum Grav. **27**, 194002 (2010).

[100] M. Kramer et al., "Strong-field gravity tests with the double pulsar," Phys. Rev. X **11**, 041050 (2021).

[101] C. Rovelli, *Quantum Gravity* (Cambridge University Press, 2004).

[102] T. Thiemann, *Modern Canonical Quantum General Relativity* (Cambridge University Press, 2007).

[103] J. F. Barbero, "Real Ashtekar variables for Lorentzian signature space-times," Phys. Rev. D **51**, 5507 (1995); G. Immirzi, "Real and complex connections for canonical gravity," Class. Quantum Grav. **14**, L177 (1997).

[104] L. Modesto, "Semiclassical loop quantum black hole," Int. J. Theor. Phys. **49**, 1649 (2010).

[105] D.-W. Chiou, "Phenomenological loop quantum geometry of the Schwarzschild black hole," Phys. Rev. D **78**, 064040 (2008).

[106] J. Olmedo, S. Saini, and P. Singh, "From black holes to white holes: a quantum gravitational, symmetric bounce," Class. Quantum Grav. **34**, 225011 (2017).

[107] S. D. Mathur, "The information paradox: a pedagogical introduction," Class. Quantum Grav. **26**, 224001 (2009).

[108] O. Lunin and S. D. Mathur, "AdS/CFT duality and the black hole information paradox," Nucl. Phys. B **623**, 342 (2002).

[109] O. Lunin and S. D. Mathur, "Statistical interpretation of Bekenstein entropy for systems with a stretched horizon," Phys. Rev. Lett. **88**, 211303 (2002).

[110] I. Bena and N. P. Warner, "Black holes, black rings and their microstates," Lect. Notes Phys. **755**, 1 (2008).

[111] I. Bena and S. Giusto, "Black holes, black rings, and microstate geometries," Fortschr. Phys. **60**, 1019 (2012).

[112] I. Bena, S. Giusto, R. Russo, M. Shigemori, and N. P. Warner, "Habemus superstratum! A constructive proof of the existence of superstrata," JHEP **1505**, 110 (2015).

[113] V. Jejjala, O. Madden, S. F. Ross, and G. Titchener, "Non-supersymmetric smooth geometries and D1-D5-P bound states," Phys. Rev. D **71**, 124030 (2005).

[114] I. Bena, P. Heidmann, and D. Turton, "Microstate geometries from gauged supergravity in three dimensions," JHEP **2010**, 162 (2020).

[115] S. Weinberg, "Ultraviolet divergences in quantum theories of gravitation," in *General Relativity: An Einstein Centenary Survey*, ed. S. Hawking and W. Israel (Cambridge University Press, 1979).

[116] M. Reuter and F. Saueressig, *Quantum Gravity and the Functional Renormalization Group: The Road towards Asymptotic Safety* (Cambridge University Press, 2019).

[117] M. Reuter and H. Weyer, "Renormalization group improved gravitational actions: a Brans-Dicke approach," Phys. Rev. D **69**, 104022 (2004).

[118] K. Falls and D. F. Litim, "Black hole thermodynamics under the microscope," Phys. Rev. D **89**, 084002 (2014).

[119] A. Bonanno, A. Eichhorn, H. Gies, J. M. Pawlowski, R. Percacci, M. Reuter, F. Saueressig, and G. P. Vacca, "Critical reflections on asymptotically safe gravity," Front. Phys. **8**, 269 (2020).

[120] V. Cardoso, J. L. Costa, K. Destounis, P. Hintz, and A. Jansen, "Quasinormal modes and strong cosmic censorship," Phys. Rev. Lett. **120**, 031103 (2018).

[121] P. Hintz and A. Vasy, "The global non-linear stability of the Kerr–de Sitter family of black holes," Acta Math. **220**, 1 (2018).

[122] E. Berti, V. Cardoso, and C. M. Will, "On gravitational-wave spectroscopy of massive black holes with the space interferometer LISA," Phys. Rev. D **73**, 064030 (2006).

[123] M. Isi, M. Giesler, W. M. Farr, M. A. Scheel, and S. A. Teukolsky, "Testing the no-hair theorem with GW150914," Phys. Rev. Lett. **123**, 111102 (2019).

[124] V. Cardoso, S. Hopper, C. F. B. Macedo, C. Palenzuela, and P. Pani, "Gravitational-wave signatures of exotic compact objects and of quantum corrections at the horizon scale," Phys. Rev. D **94**, 084031 (2016).